LETTER

doi:10.1038/nature13989

Tissue-resident macrophages originate from yolk-sac-derived erythro-myeloid progenitors

Elisa Gomez Perdiguero[1]*, Kay Klapproth[2]*, Christian Schulz[1], Katrin Busch[2], Emanuele Azzoni[3], Lucile Crozet[1], Hannah Garner[1], Celine Trouillet[1], Marella F. de Bruijn[3], Frederic Geissmann[1]§ & Hans-Reimer Rodewald[2]§

Most haematopoietic cells renew from adult haematopoietic stem cells (HSCs)[1–3], however, macrophages in adult tissues can self-maintain independently of HSCs[4–7]. Progenitors with macrophage potential *in vitro* have been described in the yolk sac before emergence of HSCs[8–13], and fetal macrophages[13–15] can develop independently of *Myb*[4], a transcription factor required for HSC[16], and can persist in adult tissues[4,17,18]. Nevertheless, the origin of adult macrophages and the qualitative and quantitative contributions of HSC and putative non-HSC-derived progenitors are still unclear[19]. Here we show in mice that the vast majority of adult tissue-resident macrophages in liver (Kupffer cells), brain (microglia), epidermis (Langerhans cells) and lung (alveolar macrophages) originate from a *Tie2*$^{+}$ (also known as *Tek*) cellular pathway generating *Csf1r*$^{+}$ erythro-myeloid progenitors (EMPs) distinct from HSCs. EMPs develop in the yolk sac at embryonic day (E) 8.5, migrate and colonize the nascent fetal liver before E10.5, and give rise to fetal erythrocytes, macrophages, granulocytes and monocytes until at least E16.5. Subsequently, HSC-derived cells replace erythrocytes, granulocytes and monocytes. Kupffer cells, microglia and Langerhans cells are only marginally replaced in one-year-old mice, whereas alveolar macrophages may be progressively replaced in ageing mice. Our fate-mapping experiments identify, in the fetal liver, a sequence of yolk sac EMP-derived and HSC-derived haematopoiesis, and identify yolk sac EMPs as a common origin for tissue macrophages.

Csf1r-expressing cells in the mouse embryo give rise to tissue-resident macrophages in adult tissues[4]. To identify in the developing embryo the site of origin of *Csf1r*-expressing cells, we performed time course analyses by constitutive (*Csf1r*^{iCre}) and inducible (*Csf1r*^{MeriCreMer}) fate-mapping of cells in the yolk sac, head, limbs, caudal region and fetal liver (Fig. 1a and Extended Data Fig. 1). Progenitors, defined as Kit^{+}CD45^{lo} (ref. 12) (gate R1 in Fig. 1b), were first detected in *Csf1r*^{iCre}*Rosa26*^{YFP} embryos in the yolk sac from 16–18 somite pairs (sp) stage onwards (E8.5, Fig. 1b, and Extended Data Fig. 1a–c). *Csf1r*^{iCre} YFP^{+}Kit^{-}CD45^{+} cells (gate R2 in Fig. 1b), characterized in Fig. 2 as myeloid cells, were detected in the yolk sac at 20–25 sp (E9, Fig. 1b), and subsequently in the caudal and head regions of the embryo from E9.5, and the fetal liver from E10.5 onwards (Extended Data Fig. 1a–d). To discriminate migration of YFP^{+} cells from *de novo* labelling, we induced YFP expression in *Csf1r*^{MeriCreMer}*Rosa26*^{YFP} embryos at E6.5 or E8.5. In embryos pulsed at E6.5, YFP^{+} cells were not detected (Extended Data Fig. 2a, b). When pulsed at E8.5, *Csf1r*^{MeriCreMer} YFP^{+}Kit^{+}CD45^{lo} progenitors were detected between E9.5–11.5 in the yolk sac, and in the fetal liver from E10.5 (Fig. 1c, d). In the fetal liver, numbers of YFP^{+}Kit^{+}CD45^{lo} progenitors increased threefold from E10.5 to E11.5, at which time they were 25-fold more numerous in the fetal liver than in the yolk sac (Fig. 1d). At E8.5, all YS *Csf1r*^{iCre} YFP^{+}Kit^{+}CD45^{lo} progenitors expressed AA4.1, an antigen expressed on early haematopoietic progenitors[12] (Extended Data Fig. 1e). *Csf1r*^{MeriCreMer} YFP^{+}AA4.1^{+}Kit^{+}CD45^{lo} cells were also present in the yolk sac from E9.5 to E10.5, and in the fetal liver from E10.5 (Fig. 1e). These progenitors were undetectable at E10.5 in the aorta-gonado-mesonephros (AGM) region (Fig. 1e), indicating they do not originate within the embryo proper.

Together, these fate-mapping experiments demonstrate that yolk-sac-derived progenitors colonize the liver primordium, as proposed earlier[8,20,21], and their expression of AA4.1 suggests that they represent erythro-myeloid progenitors (EMPs)[12]. In *in vitro* colony-forming assays, the AA4.1^{+} population contained most of the total E9 yolk sac colony-forming-units-culture (CFU-C 266 ± 137 vs 296 ± 75, mean ± standard deviation (s.d.)). Frequencies and distributions of different CFU-C, that is, erythroid (E)/megakaryocyte (Mk) (E/Mk), granulocyte/macrophage (G/M), and G,M,E, and/or Mk (Mix) potential, were comparable between overall AA4.1^{+} and *Csf1r*^{iCre} YFP^{+} AA4.1^{+} progenitors (Fig. 2a, Extended Data Fig. 3). Moreover, in the E12.5 fetal liver, the CFU potential of overall AA4.1^{+} and *Csf1r*^{MeriCreMer} YFP^{+}AA4.1^{+} cells was comparable to the yolk sac progenitors (Fig. 2a).

These results indicated that yolk-sac-derived, E8.5-labelled YFP^{+} AA4.1^{+}Kit^{+}CD45^{lo} progenitors have erythroid and myeloid potential in yolk sac and fetal liver. Next, we investigated by fate-mapping their contribution to fetal liver haematopoiesis *in vivo*. *Csf1r*^{iCre} YFP^{+} and *Csf1r*^{MeriCreMer} YFP^{+}F4/80^{bright} fetal macrophages were first detected among Kit^{-}CD45^{+} (R2 in Fig. 1b) at E10.5 in the yolk sac, liver, head and forelimbs (Fig. 2b, Extended Data Fig. 4a–c). In addition, the fetal liver from E12.5 to E16.5 contained *Csf1r*^{MeriCreMer} YFP^{+} monocytes and granulocytes (Fig. 2c). The fetal liver also contained *Csf1r*^{MeriCreMer} YFP^{+} red blood cells from E11.5 until at least E14.5 (Fig. 2d, Extended Data Fig. 4d). Red blood cells were not labelled before E11.5, indicating that, in contrast to yolk-sac-derived erythrocytes in the fetal liver, primitive erythrocytes in the yolk sac did not arise from *Csf1r*-expressing cells. Collectively, yolk-sac-derived *Csf1r*$^{+}$ progenitors contribute to fetal liver haematopoiesis by giving rise to F4/80^{bright} macrophages, monocytes, granulocytes and red blood cells.

We next investigated the transition from yolk-sac-derived to HSC-derived haematopoiesis. To trace the latter, we used *Flt3*^{Cre} which labels fetal and adult HSC-derived multipotent haematopoietic progenitors[22], and their progeny (Extended Data Fig. 5). We compared progeny of yolk-sac-derived progenitors in *Csf1r*^{MeriCreMer} mice to progeny of HSCs in *Flt3*^{Cre} mice. In the fetal liver from E14.5 to E18.5, the progenies of *Csf1r*$^{+}$ and *Flt3*$^{+}$ precursors were distinct but complemented each other (Fig. 3a). At E14.5, yolk-sac-derived CD45^{+} populations included Kit^{+} progenitors, F4/80^{bright} macrophages, and CD11b^{hi}Gr1^{+} monocytes/granulocytes (Fig. 3a, Extended Data Fig. 6a). Of note, monocytes/granulocytes were present in *Myb*-deficient fetal liver (Fig. 3a). *Csf1r*^{MeriCreMer} YFP^{+} macrophages remained detectable throughout fetal development, and were not replaced by *Flt3*^{Cre} YFP^{+} cells. However, yolk-sac-derived Kit^{+} cells and myeloid cells were no longer detectable by E16.5 and E18.5, respectively (Fig. 3a). In contrast, *Flt3*^{Cre} YFP^{+}Kit^{+}

[1]Centre for Molecular and Cellular Biology of Inflammation (CMCBI), King's College London, London SE1 1UL, UK. [2]Division of Cellular Immunology, German Cancer Research Center (DKFZ), D-69120 Heidelberg, Germany. [3]MRC Molecular Haematology Unit, Weatherall Institute of Molecular Medicine, John Radcliffe Hospital University of Oxford, Oxford OX3 9DS, UK.
*These authors contributed equally to this work.
§These authors jointly supervised this work.

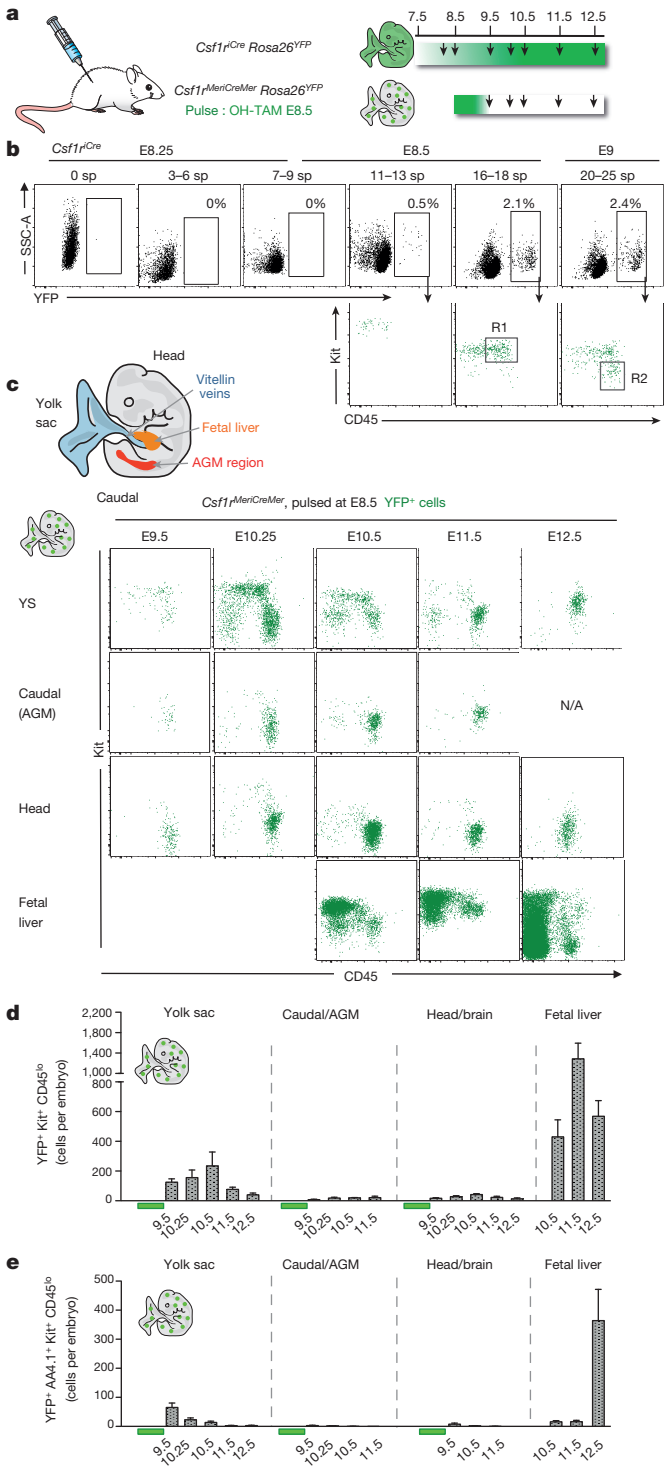

Figure 1 | E8.5 *Csf1r*$^{+}$ progenitors originate in the yolk sac and expand in the fetal liver. **a**, Fate-mapping analysis of *Csf1r*-expressing cells. Arrows indicate time points for analysis, and green shades the genetic labelling period. **b**, YFP expression on live cells from *Csf1r*^{iCre}*Rosa26*^{YFP} yolk sac (YS), separated by somite pairs between E8.25 and E9 (0 sp, $n = 3$; 3–6 sp, $n = 3$; 7–9 sp, $n = 5$; 11–13 sp, $n = 3$; 16–18 sp, $n = 4$; 20–25 sp, $n = 4$) (upper panels), and Kit and CD45 expression on YFP^{+} cells (lower panels). R1 indicates Kit^{+}CD45^{lo}, and R2 indicates Kit^{-}CD45^{+} cells. **c**, Schematic representation of sites analysed in mouse embryos: YS, AGM region, fetal liver and head. Kit and CD45 phenotype of YFP^{+} cells from *Csf1r*^{MeriCreMer} *Rosa26*^{YFP} embryos pulsed with OH-TAM at E8.5 (E9.5, $n = 3$; E10.25, $n = 3$; E10.5, $n = 4$; E11.25, $n = 4$; E12.5, $n = 9$). **d**, Number of YFP^{+}Kit^{+}CD45^{lo} cells (R1 in panel **b**) per organ or region (mean ± s.e.m.) in *Csf1r*^{MeriCreMer} *Rosa26*^{YFP} embryos pulsed at E8.5 (Source Data Table for Fig. 1). **e**, Number of YFP^{+}AA4.1^{+}Kit^{+}CD45^{lo} cells per embryonic region and time points (mean ± s.e.m.) in *Csf1r*^{MeriCreMer} *Rosa26*^{YFP} embryos pulsed at E8.5 (Source Data Table for Fig. 1). See also Supplementary Table 1 and Extended Data Figs 1 and 2.

cells, and CD11b^{hi}Gr1^{+} granulocytes/ monocytes increased in numbers between E14.5 and E18.5 (Fig. 3a–c). The progenies of *Csf1r*$^{+}$ progenitors and *Flt3*$^{+}$ progenitors were also distinct during development in the lung and skin (Extended Data Fig. 6b, c). Quantitative analyses in fetal and adult tissues indicated that *Flt3*^{Cre} YFP labelling of Kit^{+} progenitors preceded that of monocytes/granulocytes, with 80% of progenitors labelled at E18.5, and 80% of monocytes at postnatal day 8 (P8) (Fig. 3b). In contrast, *Flt3*^{Cre} YFP labelling plateaued at 14% for adult liver F4/80^{bright} Kupffer cells, at 2% for CD45^{lo} brain microglia, and 30% for epidermal Langerhans cells up to one year of life (Fig. 3b). In contrast, *Flt3*^{Cre} YFP labelling of CD45^{+} F4/80^{+} brain macrophages, and lung alveolar macrophages was 16% in 12-week-old adults but increased progressively over time to reach 40% in one-year-old mice (Fig. 3b).

Altogether, these data indicate that *Flt3*^{Cre} YFP^{+}Kit^{+} progenitors and monocytes account for only minor fractions of microglia, Kupffer cells, alveolar macrophages and Langerhans cells in young adults. To investigate whether the presence of these adult *Flt3*^{Cre} YFP^{+}F4/80^{bright} macrophages corresponds to their HSC origin, we performed non-myeloablative transplantations of YFP^{+} long-term-HSCs (LT-HSCs) from adult wild-type bone marrow into *Rag2*$^{-/-}$$\gamma_c$$^{-/-}$*Kit*$^{W/Wv}$ recipients[23] (Extended Data Fig. 7). Eight weeks after transplantation, the vast majority of HSCs, myeloid progenitors, monocytes and F4/80^{lo} tissue myeloid cells in the recipients were of donor HSC origin. In contrast, only 7% of F4/80^{bright} macrophages in spleen, 2% in liver, 5% in lung, 13% in pancreas, 2% in epidermis and 0% in the brain were donor-derived. Thus, recruitment of HSC-derived precursors is not a major mechanism for the maintenance of F4/80^{bright} macrophages in these tissues.

Collectively, these findings reveal that the transition from yolk-sac- to HSC-derived haematopoiesis occurs late in fetal development for monocytes (E14.5) and granulocytes (E16.5), and suggest that HSC-derived progenitors only marginally replace yolk-sac-derived microglia in the brain, Kupffer cells in the liver, Langerhans cells in the epidermis, although alveolar macrophages and brain CD45^{+}F4/80^{+} macrophages may undergo progressive replacement with age.

Labelling efficiency of most tissue-resident macrophage populations in adult *Csf1r*^{MeriCreMer}*Rosa26*^{YFP} mice pulse-labelled with 4-hydroxytamoxifen (OH-TAM) at E8.5 was low[4,24]. The strength of most genetic pulse-labelling systems is that they allow fate-mapping of cells during a specific time window, however, a weakness is the commonly incomplete labelling which could explain why a large fraction of tissue-resident macrophages remained unlabelled. Hence, based on these data we cannot formally exclude a fetal HSC origin of the unlabelled cells as suggested by others based on transfer of fetal precursors[24–26].

We thus made use of a newly generated inducible *Cre* knock-in mouse (*Tie2*^{MeriCreMer}) to track haematopoietic output from haematopoietic progenitors and HSCs *in situ* (Busch K. *et al.*, submitted). *Tie2* (also known as *Tek*) is expressed in endothelial cells, yolk sac progenitors, aorta-gonado-mesonephros region, fetal liver and adult HSCs[3]. We assessed the time window at which *Tie2*$^{+}$ cells contributed to emerging HSCs and macrophages by injecting tamoxifen at different time points (Fig. 4a, Extended Data Figs 8–10). Fetal liver E12.5 and E15.5 LT-HSCs were labelled efficiently in *Tie2*^{MeriCreMer} embryos pulsed at E6.5, E7.5 or E10.5 (Fig. 4b, Extended Data Figs 8 and 9). Yolk sac E9.5 Kit^{+}CD45^{lo} progenitors were also labelled in *Tie2*^{MeriCreMer}*Rosa26*^{YFP} embryos pulsed at E7.5 (Extended Data Fig. 10). Interestingly, fetal liver cells with a megakaryocyte-erythrocyte progenitor (MEP) phenotype, and F4/80^{bright} macrophages in yolk sac, brain, and fetal liver were labelled with high efficiency (60%) in embryos pulsed at E6.5 and E7.5, but not in embryos pulsed at E10.5 (Fig. 4b, Extended Data Fig. 8). These fate-mapping experiments directly demonstrate that E12.5 and E15.5 fetal macrophages originate from cells that express *Tie2*$^{+}$ as early as E6.5

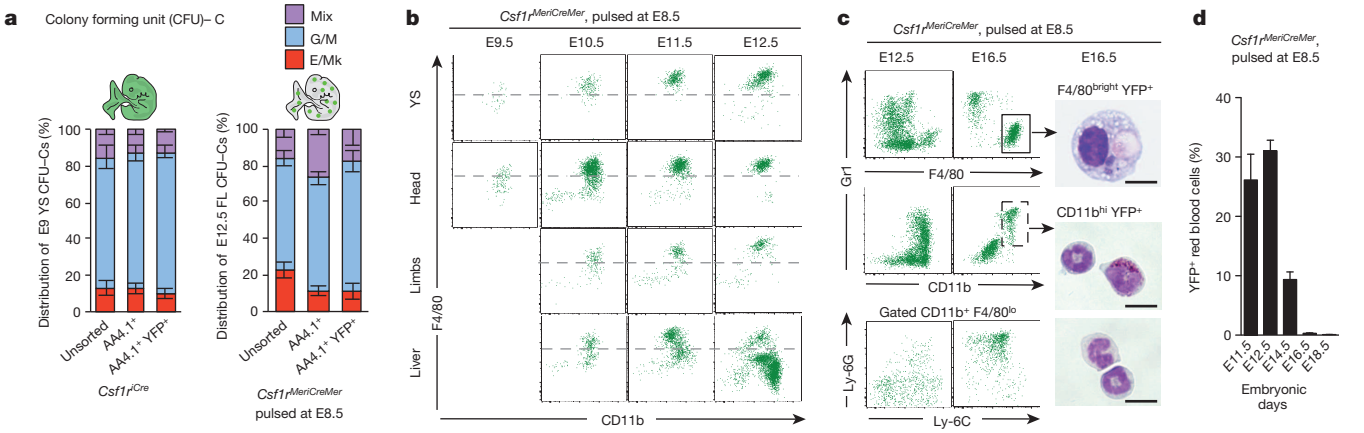

Figure 2 | E8.5 *Csf1r*$^{+}$ progenitors differentiate into myeloid cells and red blood cells in the fetal liver. **a**, Distribution of mixed (Mix), G/M, and E/Mk CFU-C from unsorted, AA4.1^{+}Kit^{+}CD45^{lo} and YFP^{+}AA4.1^{+}Kit^{+}CD45^{lo} cells from E9 yolk sac from *Csf1r*^{iCre}*Rosa26*^{YFP} and E12.5 fetal liver from *Csf1r*^{MeriCreMer}*Rosa26*^{YFP} embryos pulsed with OH-TAM at E8.5 (three independent experiments each). CFU-C erythroid and/or megakaryocyte (E/Mk); CFU-granulocyte and/or monocyte/macrophage (G/M); CFU-C mix, at least three of the following: G, E, M and Mk. See also Extended Data Fig. 3. **b**, F4/80 and CD11b expression on YFP^{+}CD45^{+} from yolk sac, head (brain for E11.5), limbs and liver of *Csf1r*^{MeriCreMer}*Rosa26*^{YFP} embryos pulsed with OH-TAM at E8.5, and analysed on E9.5 ($n = 3$), E10.5 ($n = 4$), E11.5 ($n = 4$), and E12.5 ($n = 9$); Dashed lines represent FMO (fluorescence minus one) control. See also Extended Data Fig. 4. **c**, F4/80, CD11b, Gr1, Ly-6G and Ly-6C expression in fetal liver CD45^{+}YFP^{+} cells from *Csf1r*^{MeriCreMer}*Rosa26*^{YFP} embryos pulse-labelled at E8.5, and analysed on E12.5 ($n = 9$) and E16.5 ($n = 14$). May-Grünwald-Giemsa stained cytospin preparations of fetal liver YFP^{+}F4/80^{bright} and YFP^{+}CD11b^{hi} cells sorted from E16.5 *Csf1r*^{MeriCreMer}*Rosa26*^{YFP} embryos pulsed with OH-TAM at E8.5. See also Extended Data Fig. 6a for sorted cells from E14.5 *Csf1r*^{MeriCreMer} embryos. Scale bar, 10 μm. **d**, YFP labelling efficiency (%) among red blood cells in fetal liver from *Csf1r*^{MeriCreMer}*Rosa26*^{YFP} embryos pulsed with OH-TAM at E8.5, mean ± s.e.m. (E11.5, $n = 4$; E12.5, $n = 9$; E14.5, $n = 5$; E16.5, $n = 11$; E18.5, $n = 4$; see Source Data Table Fig. 3).

and, importantly, before E9.5, and strongly support the notion that fetal liver erythro-myeloid progenitors, and all fetal tissue macrophages up to E15.5 are of yolk sac origin.

In adult mice pulsed at embryonic stages (E7.5, or E8.5, or E9.5 or E10.5), bone marrow HSC-derived progenitors, peripheral cells (T and B cells, and granulocytes) in the spleen, and CD11b^{hi}F4/80^{lo} myeloid cells

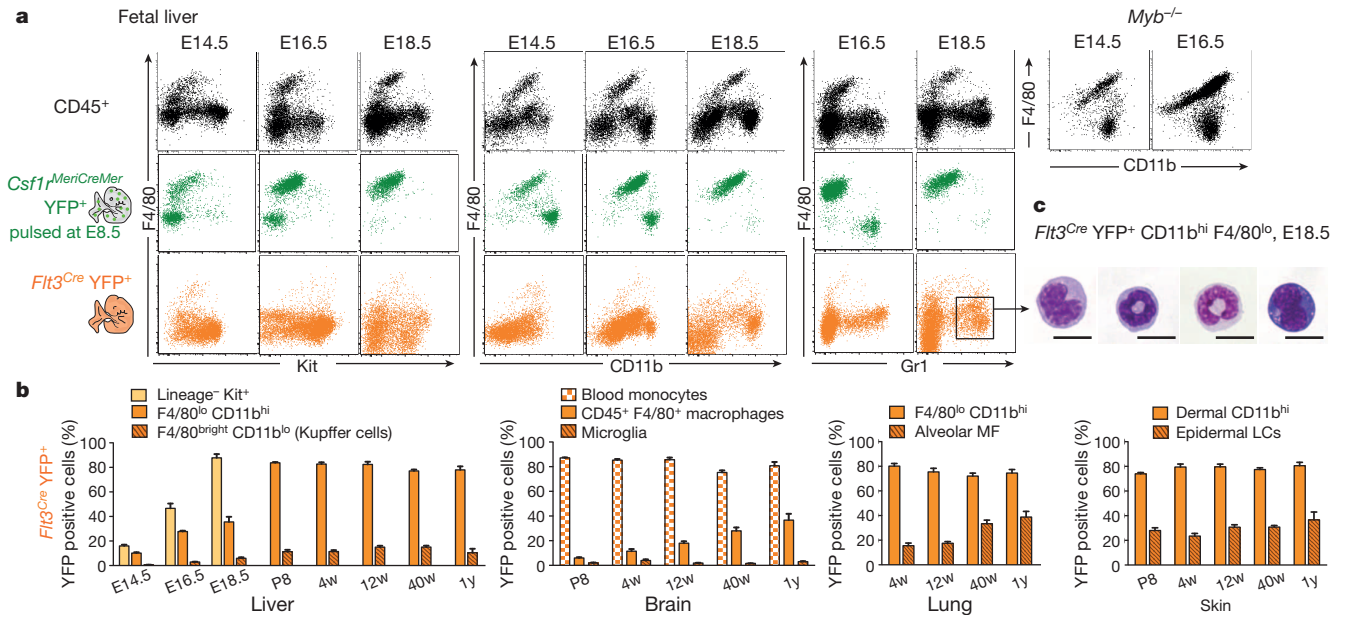

Figure 3 | Fetal liver HSC-derived *Flt3*$^{+}$ progenitors give rise to monocytes and granulocytes in late embryos and adults but do not replace yolk-sac-derived macrophages. **a**, F4/80, Kit, CD11b and Gr1 expression on total CD45^{+} cells (black) and YFP^{+}CD45^{+} cells from *Csf1r*^{MeriCreMer} *Rosa26*^{YFP} embryos pulsed at E8.5 (green) in the fetal liver at the indicated days of embryonic development (E14.5, $n = 5$; E16.5, $n = 10$; E18.5, $n = 9$). F4/80, Kit, CD11b and Gr1 expression on YFP^{+}CD45^{+} cells from *Flt3*^{Cre}*Rosa26*^{YFP} embryos (orange) (E14.5, $n = 7$; E16.5, $n = 6$; E18.5, $n = 6$). F4/80 and CD11b expression on CD45^{+} cells in *Myb*$^{-/-}$ embryos (E14.5, $n = 4$; E16.5, $n = 7$). **b**, YFP labelling efficiency in Kit^{+}lin^{-} cells, CD11b^{hi} F4/80^{lo} cells (characterized in Extended Data Fig. 5) and F4/80^{bright} macrophages (Kupffer cells in adults) in fetal and adult *Flt3*^{Cre}*Rosa26*^{YFP} liver (first panel on the left). YFP labelling efficiency in blood monocytes, brain microglia (CD45^{lo}F4/80^{+}) and CD45^{+}F4/80^{+} brain macrophages in *Flt3*^{Cre}*Rosa26*^{YFP} pups and mice (second panel). YFP labelling efficiency in alveolar macrophages (F4/80^{bright} Siglec-F^{+} CD11b^{-}) and F4/80^{lo} CD11b^{hi} myeloid cells in *Flt3*^{Cre}*Rosa26*^{YFP} lungs (third panel). YFP labelling efficiency in epidermal Langerhans cells (LCs) and dermal CD11b^{hi} (MHC II^{+}EpCAM^{-}) myeloid cells in *Flt3*^{Cre}*Rosa26*^{YFP} skin (fourth panel, see Extended Data Fig. 6b, c). Mean ± s.e.m.; P8, $n = 3$; 4-week-old, $n = 6$; 12-week-old, $n = 11$–14; 40-week-old, $n = 7$; 1-year-old, $n = 3$, see Source Data table Fig. 3. w, week; y, year. **c**, Representative images of May-Grünwald-Giemsa stained cytospin preparations of YFP^{+}CD11b^{hi}F4/80^{lo} cells sorted from E18.5 *Flt3*^{Cre} *Rosa26*^{YFP} fetal liver. Scale bar, 10 μm.

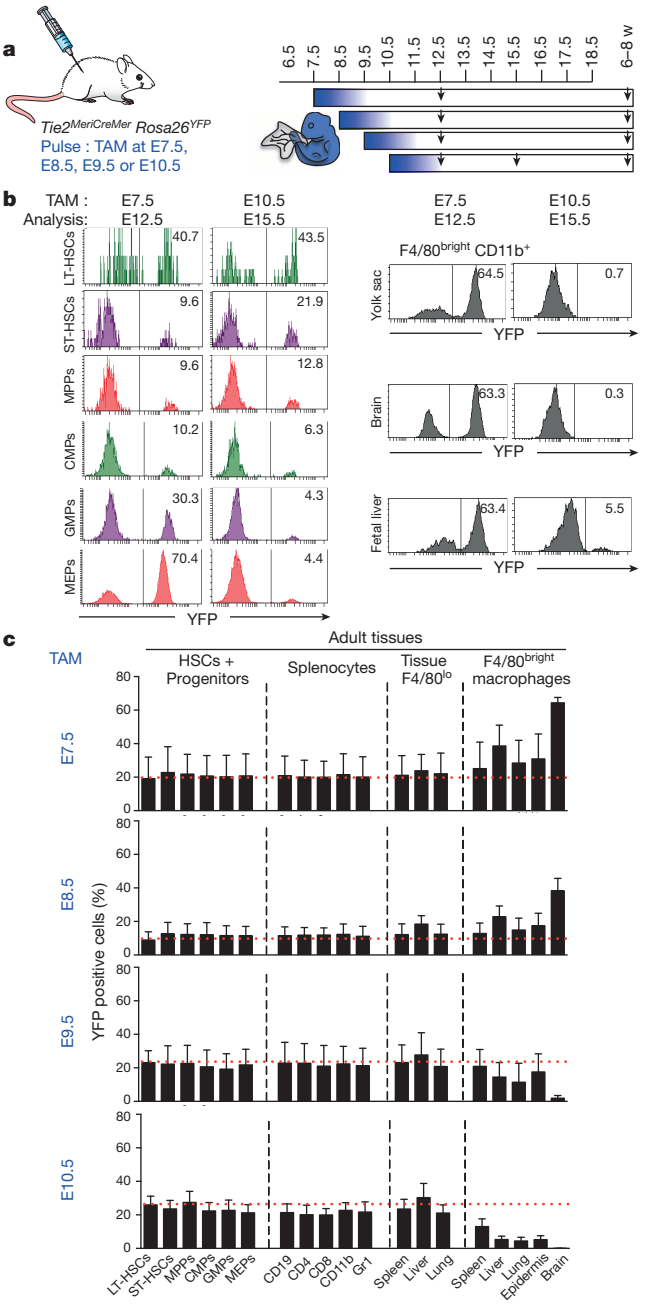

Figure 4 | Fetal macrophages and adult tissue-resident macrophages originate from *Tie2*-expressing progenitors before E10.5. **a**, Fate-mapping analysis of *Tie2*-expressing cells after tamoxifen (TAM) administration at E7.5, or E8.5, or E9.5 or E10.5. Arrows indicate time points for analysis. **b**, Flow cytometric analysis of fetal liver long-term or short-term haematopoietic stem cells (LT-HSCs, ST-HSCs), multipotent progenitors (MPPs), common myeloid progenitors (CMPs), granulocyte-monocyte progenitors (GMPs), megakaryocyte-erythrocyte progenitors (MEPs) (left panel) and of fetal macrophages (right panel) in the yolk sac, brain, and fetal liver. Time points of labelling (E7.5 ($n = 7$); E10.5 ($n = 7$)) and analysis are indicated, and for each experiment one representative analysis is shown. See Extended Data Fig. 8 for quantitative analysis. **c**, Frequencies of labelled HSCs and progenitor cells, splenocytes, and F4/80^{lo}CD11b^{hi} myeloid cells and F4/80^{bright} resident macrophages in spleen, liver lung, epidermis and brain were analysed (mean ± s.d., see Source Data Table Fig. 4) from 6–8-week-old *Tie2*^{MeriCreMer} animals pulse-labelled at E7.5 ($n = 4$), E8.5 ($n = 4$), E9.5 ($n = 4$) or E10.5 ($n = 6$).

in peripheral tissues (spleen, liver and lung) were homogenously labelled at frequencies comparable to HSC labelling, consistent with their adult HSC origin (Fig. 4c). In contrast, YFP labelling frequencies of adult tissue-resident macrophages were maximal in animals pulse-labelled at E7.5, declined at later time points and were minimal when labelled at E10.5 (Fig. 4c). The fact that adult HSCs are disconnected from resident macrophages is further underscored by the finding that resident macrophages in mice pulsed at E7.5 were labelled at higher frequencies than adult HSCs, that is, labelling efficiency did not equilibrate with mouse development. In summary, these inducible temporal analyses demonstrate that although both macrophages and HSCs originate from progenitors expressing *Tie2* as early as E6.5, adult tissue-resident macrophages in the brain (microglia), liver (Kupffer cells), lung (alveolar macrophages), skin (Langerhans cells), and (to some extent) spleen (F4/80^{bright} macrophages) develop almost exclusively from an *Tie2*-expressing progenitor pathway distinct from HSCs. These data are consistent with results from *Csf1r*^{MeriCreMer} pulse-labelling experiments (see Figs 1 and 2), with our earlier observation that resident macrophages are independent of the transcription factor *Myb*[4], and complement our data obtained in *Flt3*^{Cre}*Rosa26*^{YFP} mice (see Fig. 3).

This study demonstrates that *Myb*-independent tissue-resident macrophages[4] originate from yolk-sac-derived EMPs, characterized by expression of *Csf1r* from E8.5 (16–18 somites). The data do not distinguish whether resident macrophages originate from erythro-myeloid, granulocyte-macrophage, or macrophage only-progenitors because these potentials coexist within the yolk-sac-derived EMP population.

We also provide strong *in vivo* evidence for engraftment of yolk-sac-derived EMPs in the early fetal liver. These cells substantially contribute to the first wave of fetal liver haematopoiesis, followed later by bona fide fetal liver HSC-derived haematopoiesis[8,19,21]. Conclusions from recent studies that Langerhans cells and alveolar macrophages are not of yolk sac origin based on transfer of fetal precursors[24–26] should be interpreted in light of our findings that yolk sac EMPs expand in the fetal liver and are the main source for tissue-resident macrophages.

Under steady-state conditions, yolk-sac-derived macrophages are only marginally replaced by HSC-derived cells in the brain, liver and epidermis. It is remarkable that macrophages of yolk sac origin persist in functionally very distinct tissues, suggesting that the origin is more deterministic of the life span than the tissue location. However, some yolk-sac-derived macrophages can undergo replacement in older mice, as for lung alveolar macrophages. In a third group, exemplified by gut-associated macrophages[27], yolk-sac-derived macrophages are replaced by HSC-derived macrophages in the first weeks of post-natal life. The mechanisms responsible for the maintenance of yolk-sac-derived macrophages in certain adult tissues require further investigation. Although yolk-sac- and HSC-derived macrophages can co-exist in the same environment, and their balance be perturbed by pathology, the contributions of these developmentally distinct macrophage populations to homeostasis and inflammation remain to be characterized.

Online Content Methods, along with any additional Extended Data display items and Source Data, are available in the online version of the paper; references unique to these sections appear only in the online paper.

Received 12 April; accepted 21 October 2014.
Published online 3 December 2014.

1. Orkin, S. H. & Zon, L. I. Hematopoiesis: an evolving paradigm for stem cell biology. *Cell* **132,** 631–644 (2008).
2. Smith, L. G., Weissman, I. L. & Heimfeld, S. Clonal analysis of hematopoietic stem-cell differentiation *in vivo*. *Proc. Natl Acad. Sci. USA* **88,** 2788–2792 (1991).
3. Cumano, A. & Godin, I. Ontogeny of the hematopoietic system. *Annu. Rev. Immunol.* **25,** 745–785 (2007).
4. Schulz, C. *et al.* A lineage of myeloid cells independent of Myb and hematopoietic stem cells. *Science* **336,** 86–90 (2012).
5. Yona, S. *et al.* Fate mapping reveals origins and dynamics of monocytes and tissue macrophages under homeostasis. *Immunity* **38,** 79–91 (2013).
6. Hashimoto, D. *et al.* Tissue-resident macrophages self-maintain locally throughout adult life with minimal contribution from circulating monocytes. *Immunity* **38,** 792–804 (2013).
7. Ajami, B., Bennett, J. L., Krieger, C., Tetzlaff, W. & Rossi, F. M. Local self-renewal can sustain CNS microglia maintenance and function throughout adult life. *Nature Neurosci.* **10,** 1538–1543 (2007).

8. Palis, J., Robertson, S., Kennedy, M., Wall, C. & Keller, G. Development of erythroid and myeloid progenitors in the yolk sac and embryo proper of the mouse. *Development* **126,** 5073–5084 (1999).
9. Bertrand, J. Y. *et al.* Three pathways to mature macrophages in the early mouse yolk sac. *Blood* **106,** 3004–3011 (2005).
10. Lux, C. T. *et al.* All primitive and definitive hematopoietic progenitor cells emerging before E10 in the mouse embryo are products of the yolk sac. *Blood* **111,** 3435–3438 (2008).
11. Kierdorf, K. *et al.* Microglia emerge from erythromyeloid precursors via Pu.1- and Irf8-dependent pathways. *Nature Neurosci.* **16,** 273–280 (2013).
12. Bertrand, J. Y. *et al.* Characterization of purified intraembryonic hematopoietic stem cells as a tool to define their site of origin. *Proc. Natl Acad. Sci. USA* **102,** 134–139 (2005).
13. Moore, M. A. & Metcalf, D. Ontogeny of the haemopoietic system: yolk sac origin of *in vivo* and *in vitro* colony forming cells in the developing mouse embryo. *Br. J. Haematol.* **18,** 279–296 (1970).
14. Herbomel, P., Thisse, B. & Thisse, C. Ontogeny and behaviour of early macrophages in the zebrafish embryo. *Development* **126,** 3735–3745 (1999).
15. Takahashi, K., Yamamura, F. & Naito, M. Differentiation, maturation, and proliferation of macrophages in the mouse yolk sac: a light-microscopic, enzyme-cytochemical, immunohistochemical, and ultrastructural study. *J. Leukoc. Biol.* **45,** 87–96 (1989).
16. Sumner, R., Crawford, A., Mucenski, M. & Frampton, J. Initiation of adult myelopoiesis can occur in the absence of c-Myb whereas subsequent development is strictly dependent on the transcription factor. *Oncogene* **19,** 3335–3342 (2000).
17. Alliot, F., Godin, I. & Pessac, B. Microglia derive from progenitors, originating from the yolk sac, and which proliferate in the brain. *Brain Res. Dev. Brain Res.* **117,** 145–152 (1999).
18. Ginhoux, F. *et al.* Fate mapping analysis reveals that adult microglia derive from primitive macrophages. *Science* **330,** 841–845 (2010).
19. Frame, J. M., McGrath, K. E. & Palis, J. Erythro-myeloid progenitors: ''definitive'' hematopoiesis in the conceptus prior to the emergence of hematopoietic stem cells. *Blood Cells Mol. Dis.* **51,** 220–225 (2013).
20. Dzierzak, E. & Medvinsky, A. Mouse embryonic hematopoiesis. *Trends Genet.* **11,** 359–366 (1995).
21. Kieusseian, A., Brunet de la Grange, P., Burlen-Defranoux, O., Godin, I. & Cumano, A. Immature hematopoietic stem cells undergo maturation in the fetal liver. *Development* **139,** 3521–3530 (2012).
22. Christensen, J. L. & Weissman, I. L. Flk-2 is a marker in hematopoietic stem cell differentiation: a simple method to isolate long-term stem cells. *Proc. Natl Acad. Sci. USA* **98,** 14541–14546 (2001).
23. Waskow, C. *et al.* Hematopoietic stem cell transplantation without irradiation. *Nature Methods* **6,** 267–269 (2009).
24. Epelman, S. *et al.* Embryonic and adult-derived resident cardiac macrophages are maintained through distinct mechanisms at steady state and during inflammation. *Immunity* **40,** 91–104 (2014).
25. Hoeffel, G. *et al.* Adult Langerhans cells derive predominantly from embryonic fetal liver monocytes with a minor contribution of yolk sac–derived macrophages. *J. Exp. Med.* **209,** 1167–1181 (2012).
26. Guilliams, M. *et al.* Alveolar macrophages develop from fetal monocytes that differentiate into long-lived cells in the first week of life via GM-CSF. *J. Exp. Med.* **210,** 1977–1992 (2013).
27. Bain, C. C. *et al.* Constant replenishment from circulating monocytes maintains the macrophage pool in the intestine of adult mice. *Nature Immunol.* **15,** 929–937 (2014).

Supplementary Information is available in the online version of the paper.

Acknowledgements The authors are indebted to J. Pollard, University of Edinburgh for the *Csf1r* reporter strains, J. Frampton, University of Birmingham for the *Myb*-deficient animals, and T. Boehm, Max Planck Institute, Freiburg for the *Flt3*^{Cre} strain. The authors also thank A. McGuigan and the staff of the Biological Service Unit at King's College London, S. Heck and the Biomedical Research Centre at King's Health Partners, S. Woodcock and the staff of the Viapath haematology laboratory in Guy's hospital and S. Schäfer and T. Arnsperger for technical assistance at the German Cancer Research Center. This work was supported by a Wellcome Trust Senior Investigator award (WT101853MA) and ERC Investigator award (2010-StG-261299) from the European Research Council to F.G. and an ERC Investigator award (Advanced Grant 233074), SFB 938 project L, and SFB 873 project B11 to H.-R.R.

Author Contributions E.G.P. and F.G. designed the study and wrote the manuscript. E.G.P., C.S., L.C., H.G. and C.T. performed fate-mapping experiments and E.G.P. and F.G. designed experiments and analysed the data. K.B. and H.-R.R. generated the *Tie2*^{MeriCreMer} strain and K.K., K.B. and H.-R.R. designed, performed and analysed fate-mapping experiments. E.A. and E.G.P. performed the CFU assays and E.A., E.G.P., F.G. and M.F.d.B. analysed and interpreted the experimental data. All authors contributed to the manuscript.

Author Information Reprints and permissions information is available at www.nature.com/reprints. The authors declare no competing financial interests. Readers are welcome to comment on the online version of the paper. Correspondence and requests for materials should be addressed to F.G. (frederic.geissmann@kcl.ac.uk).

METHODS

Animals. *Myb*$^{-/-}$ (ref. 28), *Csf1r*^{MeriCreMer} (ref. 29), *Csf1r*^{iCre} (ref. 30), *Flt3*^{Cre} (ref. 31), *Rag2*$^{-/-}\gamma_c^{-/-}$*Kit*$^{W/Wv}$ (ref. 23) and *Rosa26*^{YFP} reporter[32] mice have been previously described. *Rag2*$^{-/-}\gamma_c^{-/-}$*Kit*$^{W/Wv}$ were on a mixed genetic background[23], *Csf1r*^{MeriCreMer} and *Csf1r*^{iCre} mice were on FVB background, other mice were on C57BL/6 (CD45.2) background.

Csf1r^{MeriCreMer} and *Csf1r*^{iCre} mice were generated and provided by J. W. Pollard. *Myb*$^{-/-}$ mice were generated and provided by J. Frampton. *Flt3*^{Cre} mice were generated by C. Bleul and provided by T. Boehm and S. E. Jacobsen. *Rosa26*^{YFP} (B6.129X1-Gt(ROSA)26Sor$^{tm1(EYFP)Cos}$/J) reporter mice were purchased from The Jackson Laboratory. To achieve tamoxifen-dependent Cre activity in *Tie2*-expressing cells *in vivo* we generated *Tie2*^{MeriCreMer} mice. We inserted a tamoxifen inducible codon-improved recombinase (iCre)[33] flanked by two mutated oestrogen receptor sites (MeriCreMer)[34] into the first exon of the *Tie2* locus. *Tie2*^{MeriCreMer} mice were crossed to *Rosa26*^{YFP} mice to fate-map the progeny of *Tie2*-expressing cells.

No randomization method was used and the investigators were blinded to the genotype of the embryos and animals during the experimental procedure. Results are displayed as mean ± s.e.m. (Figs 1, 2 and 3) or s.d. (Fig. 4, Supplementary Table 1). All experiments included littermate controls and the minimum sample size used was 3. Embryonic development was estimated considering the day of vaginal plug formation as 0.5 days post-coitum (dpc), and staged by developmental criteria[8]. In Figs 1 and 2 and Extended Data Figs 1–4, embryos were included based on their somite number for embryonic days < E11.5, as described in ref. 8. No statistical method was used to predetermine sample size.

All animal procedures were performed in adherence to our project licence issued by the United Kingdom Home Office under the Animals (Scientific Procedures) Act 1986, or by the German regional council at the Regierungspräsidium Karlsruhe, Germany, respectively.

Genotyping. PCR genotyping of *Myb*[28], *Csf1r*^{iCre} (ref. 30), *Rag2*$^{-/-}\gamma_c^{-/-}$*Kit*$^{W/Wv}$ (ref. 23), *Csf1r*^{MeriCreMer} and *Flt3*^{Cre} mice[4] was performed according to protocols described previously. PCR genotyping of *Tie2*^{MeriCreMer} will be described elsewhere (Busch K. *et al.*, submitted).

Processing of tissues for flow cytometry. Pregnant females were killed by cervical dislocation or by exposure to CO_2. Embryos ranging from embryonic day (E) 8.25 to E18.5 were removed from the uterus and washed in 4 °C phosphate-buffered saline (PBS, Invitrogen). The yolk sac (YS) was harvested from embryos between E8.25 and E12.5. Embryos were exsanguinated through decapitation in PBS 1× 10 mM EDTA. To obtain single-cell suspensions, organs were incubated in PBS containing 1 mg ml^{-1} collagenase D (Roche), 100 U ml^{-1} DNase I (Sigma) and 3% fetal calf serum (FCS, Invitrogen) at 37 °C for 30 min.

Adult tissues (P8 to 1 year) were prepared as follows. Blood was collected by cardiac puncture from anaesthetized (isoflurane inhalation) mice. Under terminal anaesthesia, mice were perfused by gentle intracardiac injection of 10 ml prewarmed (37°C) 1× PBS. The spleen, right liver lobe and right lung lobes were collected and processed for flow cytometry. To obtain single-cell suspensions, organs were incubated for 30 min in PBS containing 1 mg ml^{-1} Collagenase D (Roche), 100 U ml^{-1} DNase I (Sigma), 2.4 mg ml^{-1} of dispase (Invitrogen) and 3% FCS (Invitrogen) at 37°C. Brains from *Tie2*^{MeriCreMer} were dissociated and incubated for 60 min at 37°C in HBSS with 0.2 mg ml^{-1} collagenase D, 20 µg ml^{-1} dispase I (Roche), and 50 U ml^{-1} DNase I (Sigma). Brain cells were resuspended in isotonic Percoll (Pharmacia) at a final density of 1.072 g ml^{-1} in HBBS containing 3% FCS. The suspension was underlayered with Percoll solution at 1.088 g ml^{-1} and overlayered with additional layers of Percoll (1.06, 1.05 and 1.03 g ml^{-1}). After centrifugation, cells were collected from 1.06 and 1.072 g ml^{-1} layers. Brains from the other strains were processed as described for the spleen. For collection of Langerhans cells from *Tie2*^{MeriCreMer} mice, epidermal sheets were prepared using an epidermis dissociation kit (Miltenyi Biotec). In the other strains, epidermal sheets were separated from the dermis after incubation for 45 min at 37°C in 2.4 mg ml^{-1} of dispase (Invitrogen) and 3% FCS (Invitrogen) and the epidermis was further digested for 30 min in PBS containing 1 mg ml^{-1} collagenase D (Roche), 100 U ml^{-1} DNase I (Sigma), 2.4 mg ml^{-1} of dispase (Invitrogen) and 3% FCS (Invitrogen) at 37°C.

Flow cytometric analysis of embryonic and adult tissues and cell sorting. Tissues were mechanically dissociated and passed through a 100 µm cell strainer (BD). Red blood cell lysis of fetal liver and adult lung and spleen was performed as described[35]. Cells were centrifuged at 320*g* for 7 min, resuspended in 4°C PBS, plated in multiwell round-bottom plates and immunolabelled for FACS analysis. After 15 min incubation with purified anti-CD16/32 (FcγRIII/II) diluted 1/50, or ChromPure mouse IgG whole molecule (Dianova) diluted 1/20 in staining buffer (1× PBS; 0.5% BSA; 2 mM ETDA), antibody mixes were added and incubated for 30 min. Where appropriate, cells were further incubated with streptavidin conjugates for 20 min. The full list of antibodies used can be found in Supplementary Table 2.

Flow cytometry was performed using a BD Biosciences FACSCanto II flow cytometer or a BD Biosciences LSR Fortessa cell analyser. All data were analysed using FlowJo 9.5 (Tree Star) or FACS Diva software (BD Bioscience).

Fetal liver, skin and lung YFP$^+$F4/80^{bright} and YFP$^+$CD11b^{hi} cells from E18.5 *Flt3*^{Cre}*Rosa26*^{YFP} embryos and from E14.5 and E16.5 *Csf1r*^{MeriCreMer}*Rosa26*^{YFP} embryos pulsed at E8.5 were sorted into FCS-coated tubes using FACSAria II for cytospin preparations.

Pulse labelling of *Csf1r*$^+$ and *Tie2*$^+$ progenitors. For genetic cell labelling we crossed tamoxifen-inducible *Csf1r*^{MeriCreMer} and *Tie2*^{MeriCreMer} transgenic mouse strains with *Rosa26*^{YFP} reporter mice. In *Csf1r*^{MeriCreMer}*Rosa26*^{YFP} embryos recombination was induced by single injection at E8.5 of 75 µg per g (body weight) of 4-hydroxytamoxifen (Sigma) into pregnant females. The 4-hydroxytamoxifen was supplemented with 37.5 µg per g (body weight) progesterone (Sigma). In *Tie2*^{MeriCreMer} *Rosa26*^{YFP} embryos recombination was induced by treatment of pregnant females by gavage at different time points (between E7.5 and E10.5) with a single dose of 2.5 mg tamoxifen (Sigma) and 1.75 mg progesterone (Sigma) to counteract the mixed oestrogen agonist effects of tamoxifen, which can result in fetal abortions.

Continuous labelling of *Csf1r*$^+$ progenitors. For fate-mapping analysis of *Csf1r*$^+$ precursors, *Csf1r*^{iCre} females were crossed with homozygous *Rosa26*^{YFP} reporter males. Indicated tissues from embryos and adult F1 mice were analysed by flow cytometry.

Fate-mapping of *Flt3*$^+$ haematopoietic progenitors. For fate-mapping analysis of *Flt3*$^+$ precursors, *Flt3*^{Cre} males (the transgene is located on the Y chromosome) were crossed to homozygous *Rosa26*^{YFP} reporter females. For adult experiments, *Flt3*^{Cre} males were blood phenotyped. Animals with YFP labelling efficiency above 60% in the lymphocytes, monocytes and granulocytes were used for experiments and female littermates were used as Cre-negative controls.

Colony forming assays. Colony-forming-unit-culture (CFU-C) assays were performed using Methocult M3434 (Stem Cell Technologies) as described in ref. 36. Embryos were collected and dissected in PBS (Gibco, Invitrogen) supplemented with 10% FCS (batch tested and obtained from Gibco), 50 U ml^{-1} penicillin, and 50 µg ml^{-1} streptomycin (Cambrex Corporation). E9 embryos were staged by somite counting. E9 yolk sac and E12 fetal livers were each pooled and incubated for 30 min at 37°C in PBS supplemented with 10% FCS, 50 U ml^{-1} penicillin, 50 µg ml^{-1} streptomycin, 1 mg ml^{-1} collagenase D (Roche) and 100 U ml^{-1} DNase I (Sigma), and dissociated by pipetting. Suspensions were washed, and viable cells were counted on the basis of trypan blue (Sigma) exclusion using a Kova hemocytometer slide.

AA4.1$^+$ progenitors were isolated by flow cytometry using using FACSAria II or FACSAria III. Labelling of cells was performed as described above using the following antibodies: CD45-APC-Cy7, Kit-PE and AA4.1-APC (Supplementary Table 2), and live cells were gated on the basis of Hoechst 33258 exclusion. Cells were collected into FCS-coated tubes and recounted before plating where possible. Gates were defined using unstained, single stained and fluorescence minus one (FMO) stained cells.

Cells were plated in duplicate in 35-mm culture dishes according to manufacturer's instructions. Cultures were grown at 37 °C with 5% CO_2 with colonies scored after 10 days.

Colonies were picked and washed once with phosphate-buffered saline (PBS; Gibco, Invitrogen) supplemented with 10% fetal calf serum (FCS; batch tested and obtained from Gibco). Cytospin preparations were stained with May-Grünwald-Giemsa method for morphological inspection of colonies (see below).

Morphological analysis of sorted cells and colonies. Cytospin preparations were performed using a Cytospin 3 (Thermo Shandon) by centrifuging (i) cells from colonies at 400 r.p.m. for 4 min (medium acceleration) or (ii) sorted cells at 500 r.p.m. for 10 min (low acceleration). Slides were air-dried for at least 30 min, and fixed for 5 min in methanol. Methanol-fixed cytospin preparations were manually stained in 50% May-Grünwald solution for 5 min, 14% Giemsa for 15 min, washed with Sorensons buffered distilled water (pH 6.8) for 5 min and rinsed with Sorensons buffered distilled water (pH 6.8). After air-drying, slides were mounted with Entellan New (Merck) and representative pictures were taken using a Nikon eclipse E6000 microscope with a Nikon Plan Fluor 60×/1.40 NA oil DIC H objective and NIS-elements BR2.30 software (Nikon).

Transplantation of HSCs without irradiation. HSC transplantation in non-irradiated *Rag2*$^{-/-}\gamma_c^{-/-}$*Kit*$^{W/Wv}$ mice was performed as described previously[23]. In brief, approximately 1000 LT-HSCs (lin$^-$Sca-1$^+$Kit$^+$CD150$^+$CD48$^-$) isolated from the bone marrow of *panRosa*^{YFP} mice, which carry a constitutively active YFP reporter allele, were injected into *Rag2*$^{-/-}\gamma_c^{-/-}$*Kit*$^{W/Wv}$ mice. Recipients were analysed 2 months after transplantation for donor/host chimaerism in blood, spleen, lung, liver, pancreas, brain and epidermis. To test the functionality of E12.5 phenotypic LT-HSCs, 10 YFP$^+$LSK CD150$^+$CD48$^-$ (phenotypic LT-HSCs) from *Tie2*^{MeriCreMer} *Rosa26*^{YFP} pulsed at E7.5 were transplanted into *Rag2*$^{-/-}\gamma_c^{-/-}$*Kit*$^{W/Wv}$ mice and blood lineages were analysed 16 weeks after.

28. Mucenski, M. L. *et al.* A functional *c-myb* gene is required for normal murine fetal hepatic hematopoiesis. *Cell* **65,** 677–689 (1991).
29. Qian, B. Z. *et al.* CCL2 recruits inflammatory monocytes to facilitate breast-tumour metastasis. *Nature* **475,** 222–225 (2011).
30. Deng, L. *et al.* A novel mouse model of inflammatory bowel disease links mammalian target of rapamycin-dependent hyperproliferation of colonic epithelium to inflammation-associated tumorigenesis. *Am. J. Pathol.* **176,** 952–967 (2010).
31. Benz, C., Martins, V. C., Radtke, F. & Bleul, C. C. The stream of precursors that colonizes the thymus proceeds selectively through the early T lineage precursor stage of T cell development. *J. Exp. Med.* **205,** 1187–1199 (2008).
32. Srinivas, S. *et al.* Cre reporter strains produced by targeted insertion of *EYFP* and *ECFP* into the *ROSA26* locus. *BMC Dev. Biol.* **1,** 4 (2001).
33. Shimshek, D. R. *et al.* Codon-improved Cre recombinase (iCre) expression in the mouse. *Genesis* **32,** 19–26 (2002).
34. Zhang, Y. *et al.* Inducible site-directed recombination in mouse embryonic stem cells. *Nucleic Acids Res.* **24,** 543–548 (1996).
35. Auffray, C. *et al.* CX3CR1^{+} CD115^{+} CD135^{+} common macrophage/DC precursors and the role of CX_3CR1 in their response to inflammation. *J. Exp. Med.* **206,** 595–606 (2009).
36. Swiers, G. *et al.* Early dynamic fate changes in haemogenic endothelium characterized at the single-cell level. *Nature Commun.* **4,** 2924 (2013).

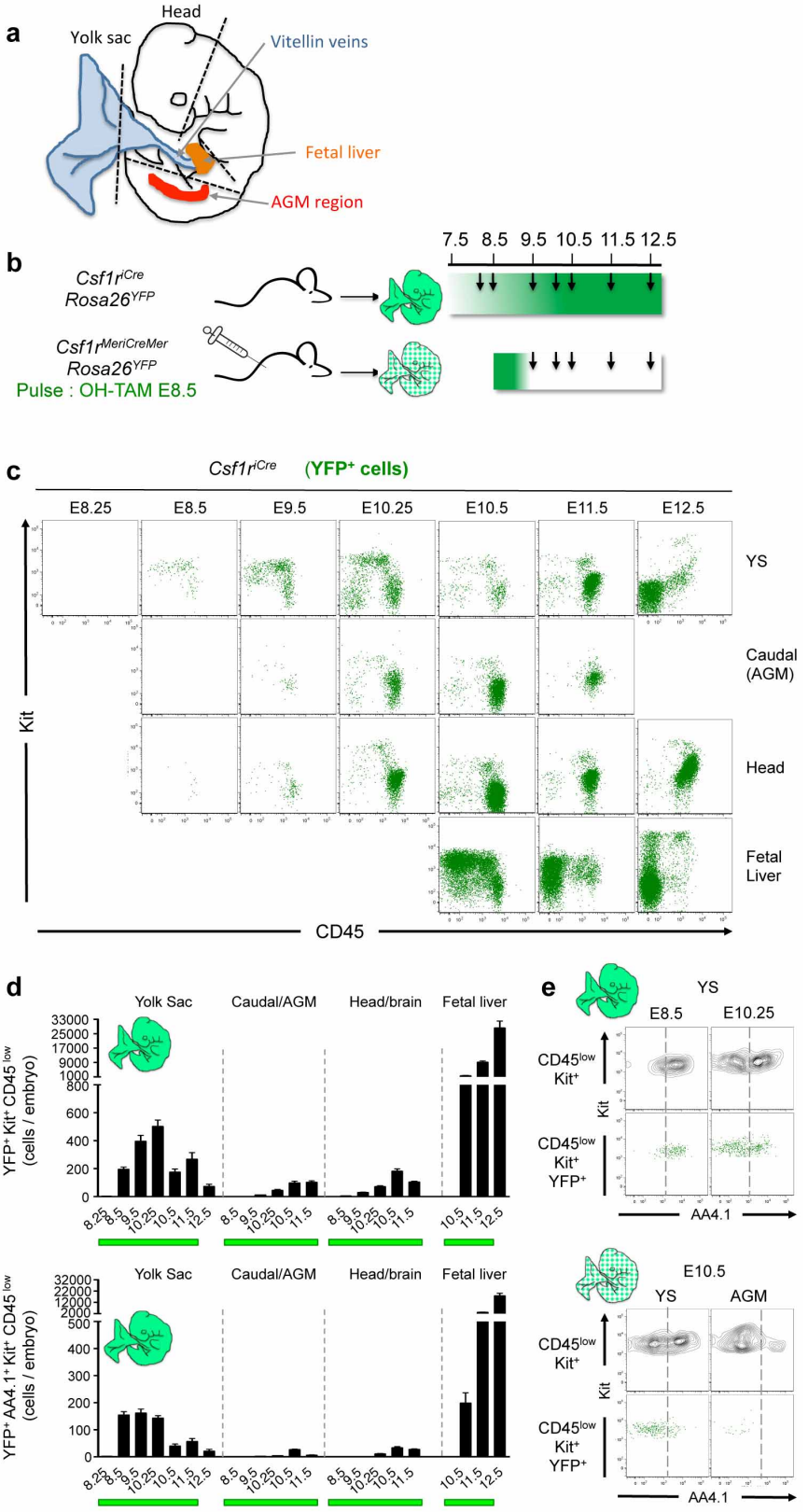

Extended Data Figure 1 | Analysis of *Csf1r* reporter expression in fetal progenitor cells in *Csf1r*^{iCre} *Rosa26*^{YFP}. **a**, Schematic representation of the different haematopoietic and non-haematopoietic sites dissected in the mouse embryos: yolk sac (YS), aorta-gonado-mesonephros (AGM) region, fetal liver and head. **b**, Experimental design for fate-mapping analysis of *Csf1r*-expressing cells. Arrows indicate analysed time points **c**, Kit and CD45 expression on YFP$^+$ cells from *Csf1r*^{iCre}*Rosa26*^{YFP} embryos (E8.25, $n = 7$; E8.5, $n = 4$; E9.25–E9.5, $n = 16$; E10.25, $n = 9$; E10.5, $n = 5$; E11.5, $n = 8$; E12.5, $n = 5$). **d**, Number of YFP$^+$Kit$^+$CD45^{lo} cells per organ/region and developmental time points (mean ± s.e.m.) in *Csf1r*^{iCre}*Rosa26*^{YFP} embryos (upper panel). Number of YFP$^+$AA4.1$^+$Kit$^+$CD45^{lo} cells per embryonic region and developmental time points (mean ± s.e.m.) in *Csf1r*^{iCre} *Rosa26*^{YFP} embryos (lower panel). **e**, AA4.1 and Kit expression on YFP$^+$ cells from *Csf1r*^{iCre}*Rosa26*^{YFP} embryos (upper panel) and from *Csf1r*^{MeriCreMer}*Rosa26*^{YFP} embryos pulsed with OH-TAM at E8.5 (lower panel).

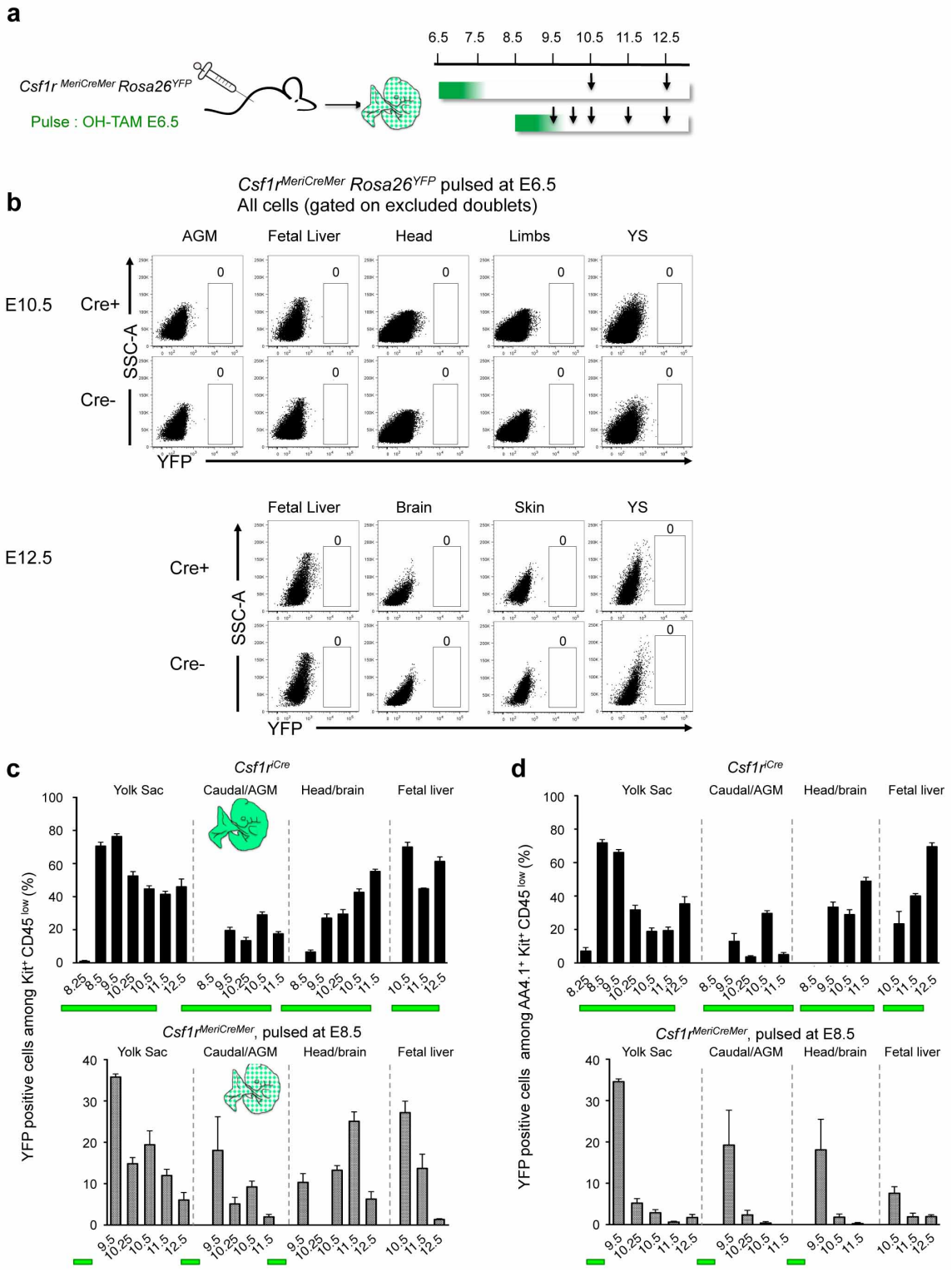

Extended Data Figure 2 | Fate-mapping analysis of *Csf1r*-expressing cells. **a**, Experimental design for fate-mapping analysis of *Csf1r*-expressing cells. Arrows indicate analysed time points. **b**, YFP expression on live cells from *Csf1r*^{MeriCreMer}*Rosa26*^{YFP} embryos pulsed at E6.5 with OH-TAM and analysed at E10.5 ($n = 2$) and E12.5 ($n = 4$). **c**, Percentage of YFP$^+$ cells among Kit$^+$CD45^{lo} cells (YFP labelling efficiency) per organ/region (mean ± s.e.m.). Upper panel, *Csf1r*^{iCre}*Rosa26*^{YFP} embryos (E8.25, $n = 7$; E8.5, $n = 4$; E9.5, $n = 16$; E10.25, $n = 9$; E10.5, $n = 5$; E11.5, $n = 8$; E12.5, $n = 5$); lower panel, *Csf1r*^{MeriCreMer}*Rosa26*^{YFP} embryos pulsed at E8.5 (E9.5, $n = 3$; E10.25, $n = 3$; E10.5, $n = 4$; E11.5, $n = 4$; E12.5, $n = 9$). **d**, Percentage of YFP$^+$ cells among AA4.1$^+$Kit$^+$CD45^{lo} cells (YFP labelling efficiency) per embryonic organ/region and developmental time points (mean ± s.e.m.). Upper panel, *Csf1r*^{iCre} *Rosa26*^{YFP} embryos; lower panel, *Csf1r*^{MeriCreMer}*Rosa26*^{YFP} embryos pulsed at E8.5.

a

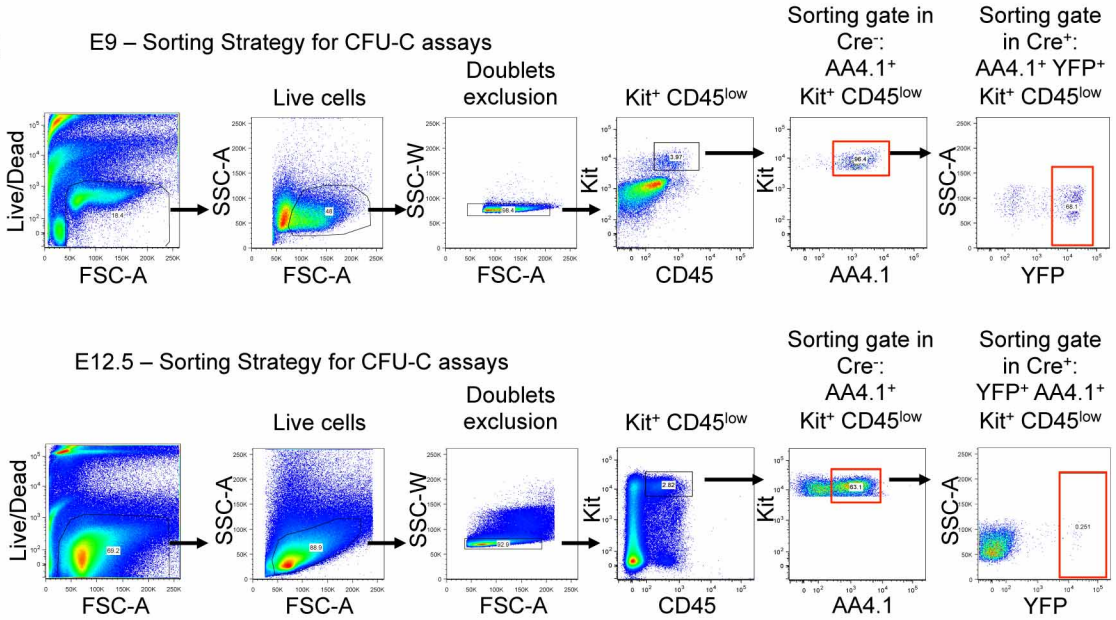

b

		Mean Frequency			
		Total CFU-C	CFU-E /Mk	CFU-G/M	CFU-Mix
E9 YS	Unsorted YS E9	1:132	1:2743	1:208	1:1167
	Kit+ CD45low AA4.1+	1:8	1:117	1:11	1:66
	Kit+ CD45low AA4.1+ *Csf1r*^{iCre} YFP+	1:10	1:121	1:13	1:121
E12.5 FL	Unsorted FL E12.5	1:177	1:894	1:288	1:1067
	Kit+ CD45low AA4.1+	1:6.5	1:63	1:11	1:27
	Kit+ CD45low AA4.1+ *Csf1r*^{MeriCreMer} YFP+	1:17.5	1:125	1:22.5	1:300

c

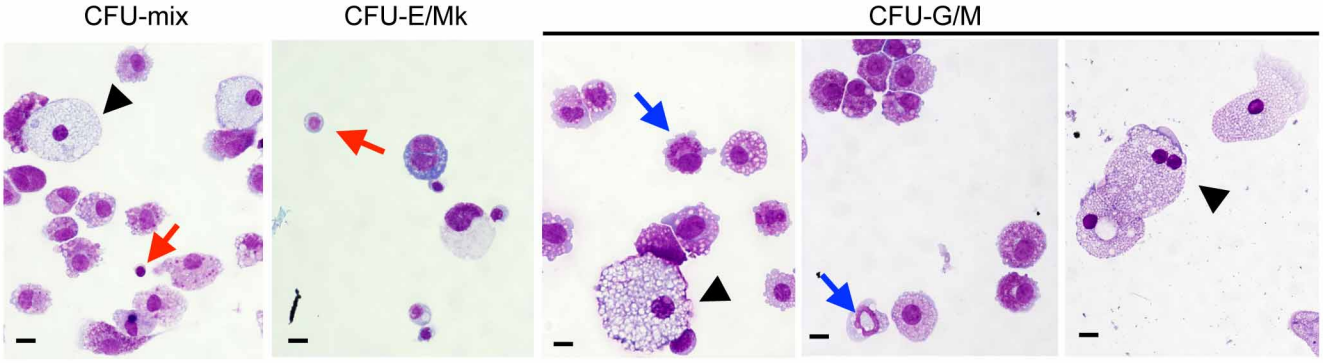

Extended Data Figure 3 | *Csf1r*$^{+}$ progenitors have erythro-myeloid potential *ex vivo*. **a**, Sorting strategy for CFU-C (colony forming unit-culture) assays for E9 *Csf1r*^{iCre}*Rosa26*^{YFP} yolk sac (upper panel) and E12.5 fetal liver from *Csf1r*^{MeriCreMer}*Rosa26*^{YFP} embryos pulsed with OH-TAM at E8.5 (lower panel). Dead cells were excluded based on Hoechst 33258 incorporation and, after doublet exclusion, cells were gated based on CD45 and Kit expression. AA4.1^{+}Kit^{+}CD45^{lo} and YFP^{+}AA4.1^{+}Kit^{+}CD45^{lo} cells were isolated from Cre^{-} and Cre^{+} embryos respectively. **b**, Mean CFU-C frequency from three independent experiments each of E9 *Csf1r*^{iCre}*Rosa26*^{YFP} YS and E12.5 fetal liver from *Csf1r*^{MeriCreMer}*Rosa26*^{YFP} embryos pulsed with OH-TAM at E8.5. CFU-erythroid and/or megakaryocyte (E/Mk); CFU-granulocyte and/or monocyte/macrophage (G/M); CFU-mix, at least three of the following: G, E, M and Mk. **c**, Morphological validation of colony types obtained from E9 yolk sac *Csf1r*^{iCre} YFP^{+}AA4.1^{+}Kit^{+}CD45^{lo} CFU-C assays. Representative images from May-Grünwald-Giemsa stained cytospin preparations of mixed, E/Mk and G/M colonies. Black arrowhead, macrophages; granulocyte pathway, blue arrows; erythroid and megakaryocyte pathway, red arrows. Scale bar, 10 µm.

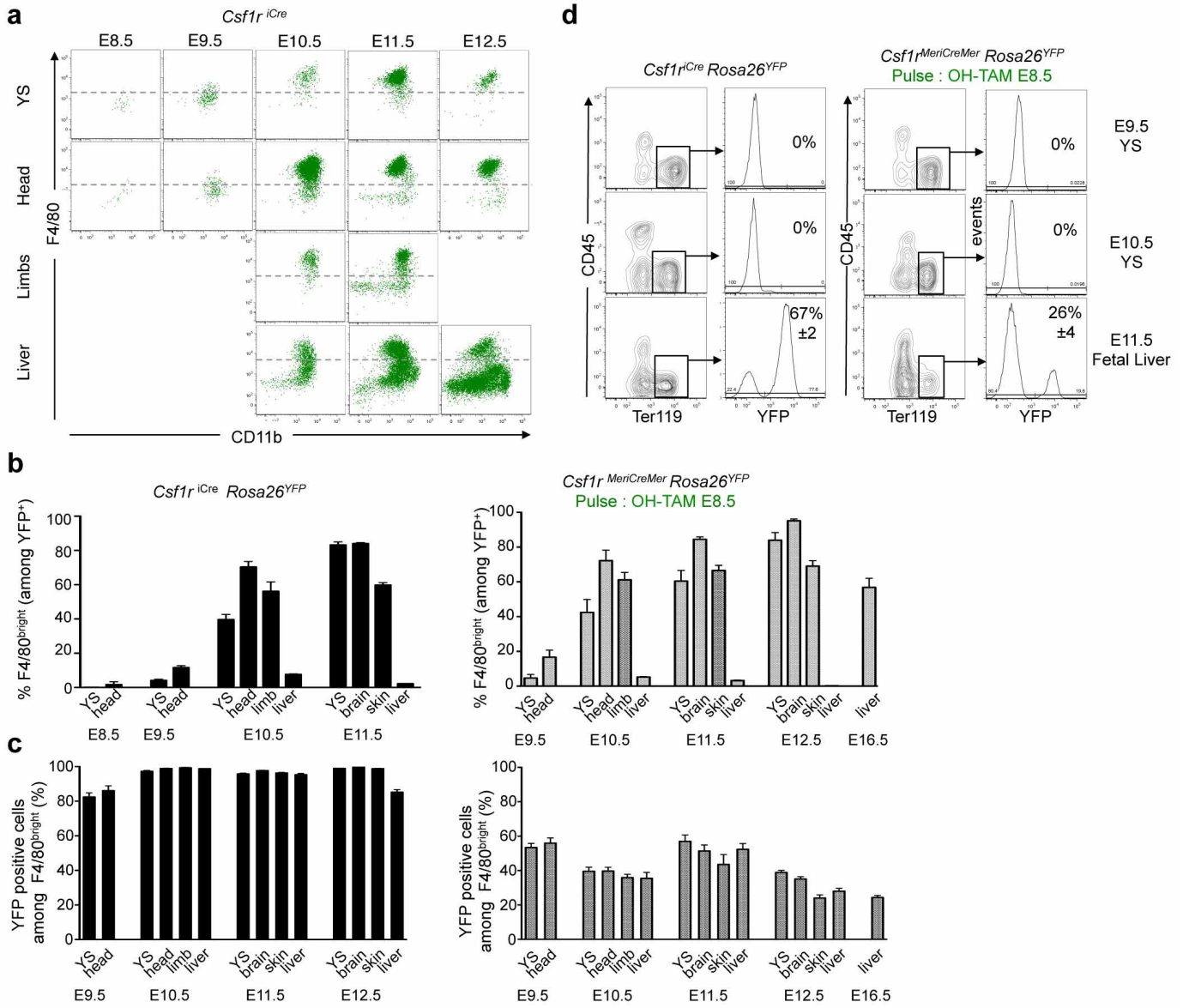

Extended Data Figure 4 | Analysis of *Csf1r* reporter expression in fetal macrophages and red blood cells in *Csf1r*^{iCre}*Rosa26*^{YFP} embryos. **a**, F4/80 and CD11b expression on YFP$^+$ CD45$^+$ from yolk sac, head (brain for E11.5), limbs and liver of *Csf1r*^{iCre}*Rosa26*^{YFP} embryos (E8.5, $n = 4$; E9.5, $n = 16$; E10.5, $n = 5$; E11.5, $n = 9$; E12.5, $n = 5$). Dashed line represents FMO (fluorescence minus one) control. **b**, Percentage of macrophages (F4/80^{bright}) among YFP$^+$ cells, mean ± s.e.m., in *Csf1r*^{iCre}*Rosa26*^{YFP} embryos (left) and in *Csf1r*^{MeriCreMer} *Rosa26*^{YFP} embryos pulsed with OH-TAM at E8.5 (right). See also Supplementary Table 1. **c**, Percentage of YFP$^+$ cells among F4/80^{bright} cells (YFP labelling efficiency) per embryonic organ/region and developmental time points (mean ± s.e.m.). Left panel, *Csf1r*^{iCre}*Rosa26*^{YFP} embryos (E8.25, $n = 7$; E8.5, $n = 5$; E9.5, $n = 15$; E10.25, $n = 9$; E10.5, $n = 5$; E11.5, $n = 9$; E12.5, $n = 5$); right panel: *Csf1r*^{MeriCreMer}*Rosa26*^{YFP} embryos pulsed at E8.5 (E9.5, $n = 3$; E10.25, $n = 3$; E10.5, $n = 4$; E11.25, $n = 4$; E12.5, $n = 9$). **d**, YFP expression in erythrocytes (CD45$^-$Ter119$^+$) from yolk sac and fetal liver of *Csf1r*^{iCre}*Rosa26*^{YFP} embryos (left) and *Csf1r*^{MeriCreMer}*Rosa26*^{YFP} embryos pulsed with OH-TAM at E8.5 (right).

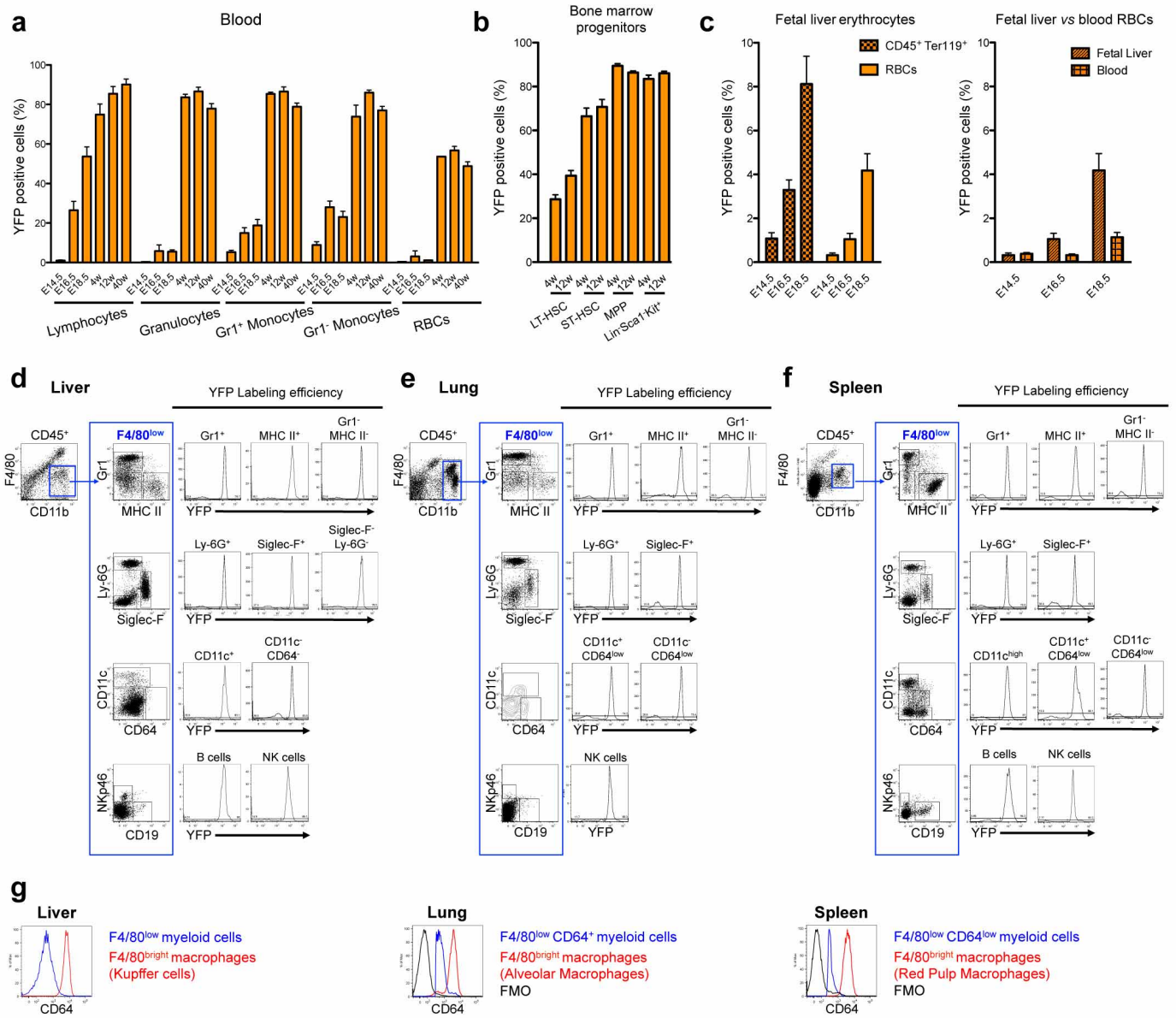

Extended Data Figure 5 | Analysis of *Flt3* reporter expression in blood leucocytes, stem/progenitor cells, fetal red blood cells, and adult liver, lung and spleen in *Flt3*^{Cre}*Rosa26*^{YFP} mice. **a**, YFP labelling efficiency in blood lineages at different embryonic and adult time points (E14.5, $n = 9$; E16.5, $n = 9$; E18.5, $n = 7$; P8, $n = 7$; 4-week-old, $n = 6$; 12-week-old, $n = 9$; 40-week-old, $n = 7$) in *Flt3*^{Cre}*Rosa26*^{YFP} mice are shown. Lymphocytes were gated as CD3$^+$/CD19$^+$, granulocytes (CD11b$^+$Gr1$^+$CD115$^-$), Gr1$^+$ monocytes (CD11b$^+$Gr1$^+$CD115$^+$), Gr1$^-$ monocytes (CD11b$^+$Gr1$^-$CD115$^+$) and red blood cells (RBCs, CD45$^-$Ter119$^+$). **b**, YFP labelling efficiency in bone marrow LT-HSCs, ST-HSCs, MPPs and Lin$^-$Sca1$^-$Kit$^+$ progenitors in 4-week-old ($n = 3$) and 12-week-old ($n = 6$) *Flt3*^{Cre}*Rosa26*^{YFP} mice. **c**, YFP labelling efficiency in fetal liver red blood cell progenitors (CD45$^+$Ter119$^+$) and red blood cells (CD45$^-$Ter119$^+$) in *Flt3*^{Cre}*Rosa26*^{YFP} mice (E14.5, $n = 5$; E16.5, $n = 5$; E18.5, $n = 7$), and comparison of YFP labelling efficiency in fetal liver and blood red blood cells in *Flt3*^{Cre}*Rosa26*^{YFP} mice at E14.5 ($n = 5$), E16.5 ($n = 5$) and E18.5 ($n = 7$). **d**, Expression of Gr1 and MHC II, Ly-6G and Siglec-F, CD11c and CD64, and Nkp46 and CD19 among F4/80^{lo}CD11b^{hi} myeloid cells in the liver. Histograms represent *Flt3*^{Cre} YFP labelling efficiency in the following defined populations: granulocytes (Gr1$^+$MHC II$^-$ or Ly-6G$^+$), eosinophils (Siglec-F$^+$), dendritic cells (CD11c$^+$), B cells (CD19$^+$) and NK cells (Nkp46$^+$) ($n = 3$). **e**, Analysis of F4/80^{lo}CD11b^{hi} myeloid cells in the lung as in **b**. **f**, Analysis of F4/80^{lo}CD11b^{hi} myeloid cells in the spleen as in **b**. **g**, Expression of CD64 in F4/80^{bright} macrophages and in F4/80^{lo} myeloid cells in the liver, lung and spleen (FMO, fluorescence minus one).

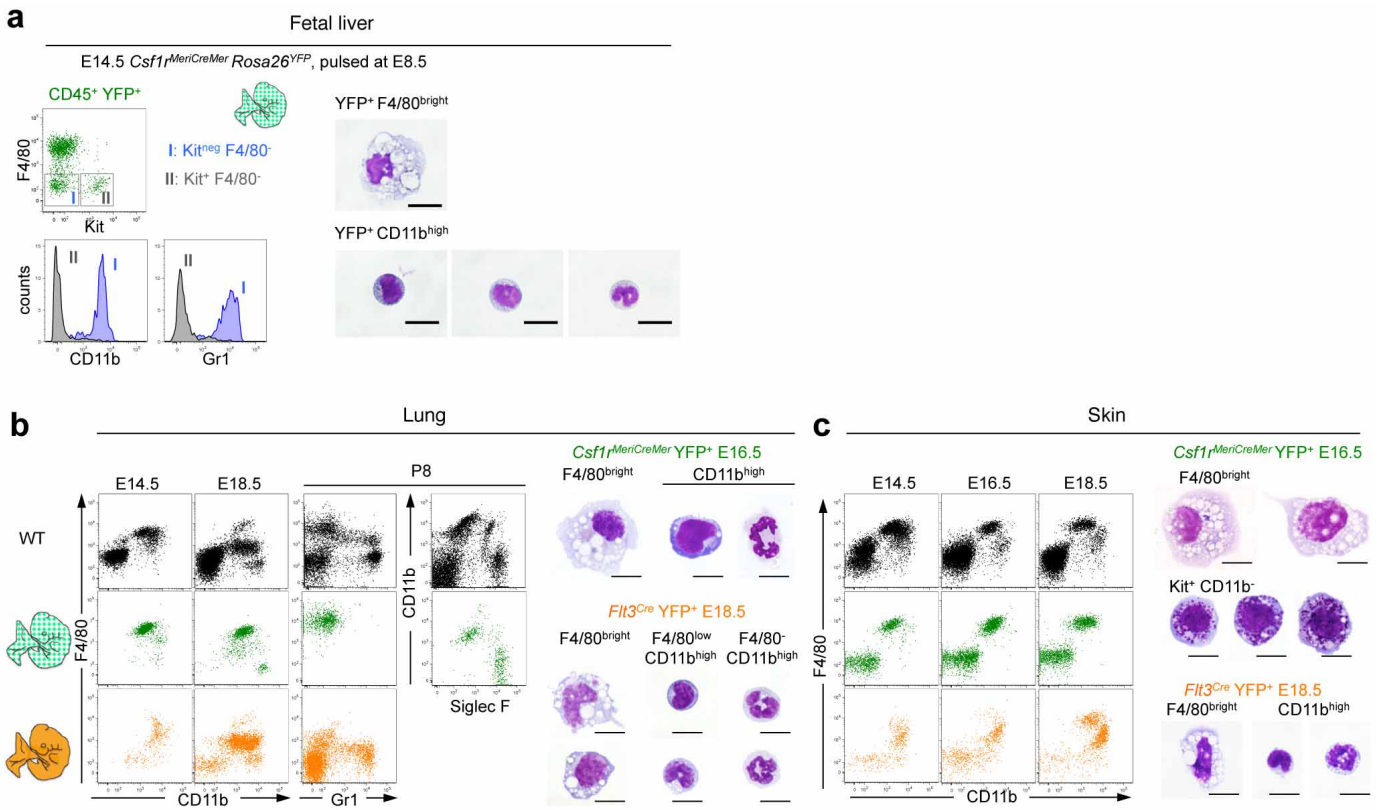

Extended Data Figure 6 | Characterization of fetal F4/80^{lo}CD11b^{hi} myeloid cells in liver, lung and skin. **a**, F4/80, Kit, CD11b and Gr1 expression on YFP$^+$CD45$^+$ cells in the fetal liver at E14.5 in *Csf1r*^{MeriCreMer}*Rosa26*^{YFP} embryos pulsed at E8.5 (left panel). Representative images of May-Grünwald-Giemsa stained cytospin preparations of fetal liver YFP$^+$F4/80^{bright} and YFP$^+$CD11b^{hi} cells sorted from E14.5 *Csf1r*^{MeriCreMer}*Rosa26*^{YFP} embryos pulsed with OH-TAM at E8.5 (right panel). Scale bar, 10 µm. **b**, **c**, F4/80, CD11b, Gr1 and Siglec F expression on CD45$^+$ cells in the embryonic and post-natal lung (**b**) and skin (**c**) in *Csf1r*^{MeriCreMer}*Rosa26*^{YFP} embryos pulsed with OH-TAM at E8.5 (green) and *Flt3*^{Cre}*Rosa26*^{YFP} embryos (orange). Representative images of May-Grünwald-Giemsa stained cytospin preparations of lung YFP$^+$F4/80^{bright} and YFP$^+$CD11b^{hi}F4/80^{lo} (**b**) and skin YFP$^+$F4/80^{bright} and YFP$^+$Kit$^+$F4/80$^-$CD11b$^-$ mast cells (**c**) sorted from E18.5 *Flt3*^{Cre}*Rosa26*^{YFP} embryos and E16.5 *Csf1r*^{MeriCreMer}*Rosa26*^{YFP} embryos pulsed with OH-TAM at E8.5. Scale bar, 10 µm.

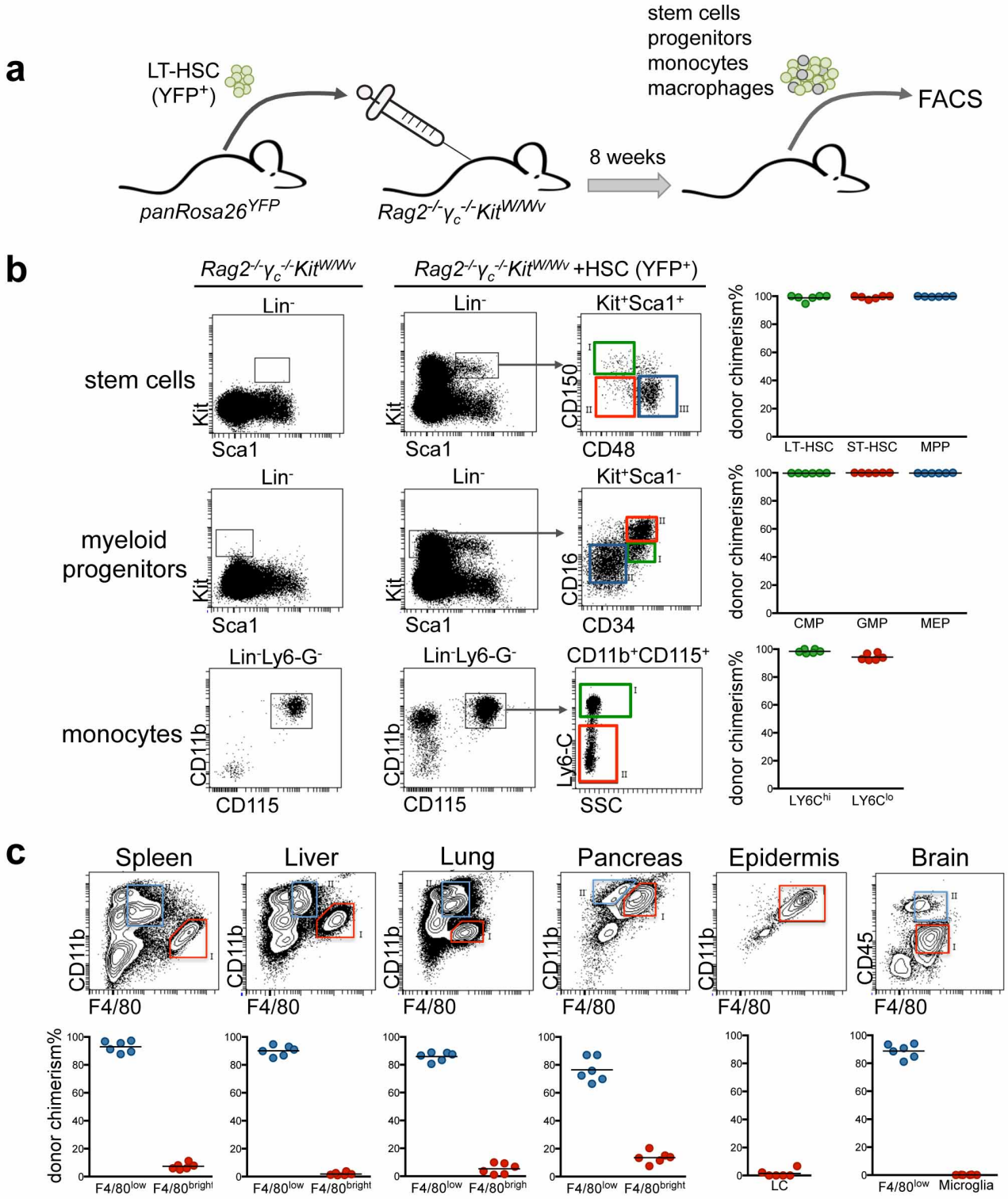

Extended Data Figure 7 | Adult BM transplantation reconstitutes the haematopoietic system but does not replace tissue-resident F4/80^{bright} macrophages. **a**, Schematic representation of transplantation experiments. LT-HSCs isolated from bone marrow of *panRosa26*^{YFP} donor mice were injected into *Rag2*$^{-/-}\gamma_c^{-/-}$*Kit*$^{W/Wv}$ recipients (approximately 1,000 cells per recipient). Eight weeks after transplantation stem cells, myeloid progenitors, monocytes and macrophages of recipient mice were analysed for donor chimaerism. **b**, Long-term or short-term haematopoietic stem cells (LT-HSCs, ST-HSCs), multipotent progenitors (MPPs), common myeloid progenitors (CMPs), granulocyte-monocyte progenitors (GMPs), megakaryocyte-erythrocyte progenitors (MEPs), and circulating Ly6C^{hi} and Ly6C^{lo} monocytes were isolated from transplanted *Rag2*$^{-/-}\gamma_c^{-/-}$*Kit*$^{W/Wv}$ mice and analysed for YFP expression. **c**, F4/80^{bright} macrophages and F4/80^{lo} myeloid cells in spleen, liver, lung, pancreas, epidermis and brain were analysed for YFP expression.

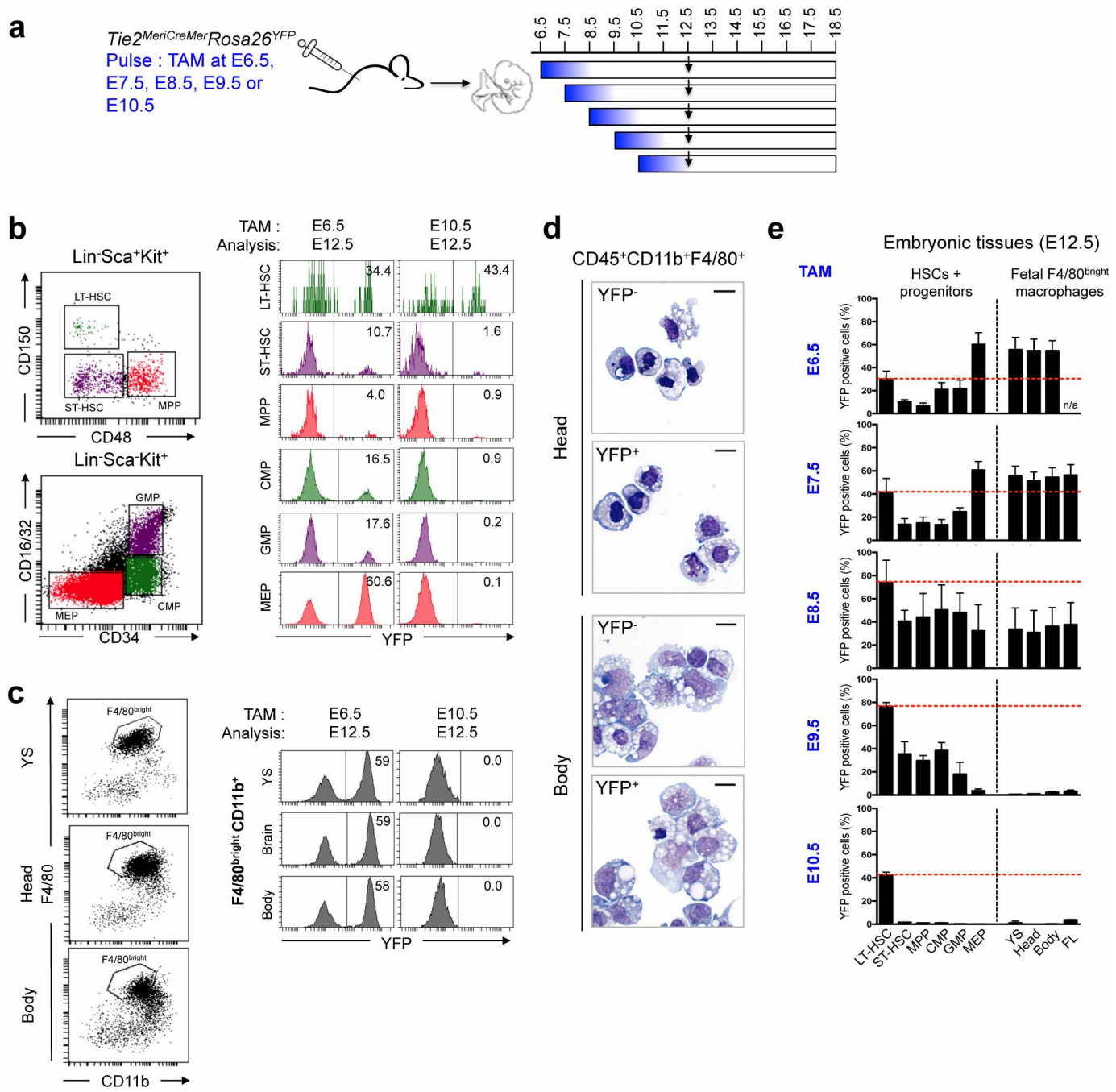

Extended Data Figure 8 | Analysis of fetal stem/progenitor cells and fetal macrophages in *Tie2*^{MeriCreMer}*Rosa26*^{YFP} embryos pulse-labelled from E6.5 to E10.5. **a**, Experimental design for fate-mapping analysis of *Tie2*^{MeriCreMer}*Rosa26*^{YFP} embryos pulse-labelled at E6.5, or E7.5, or E8.5, or E9.5 or E10.5. **b**, **c**, Representative flow cytometry of fetal liver stem/progenitor cells (**b**) and of fetal macrophages (**c**) in the yolk sac, head region, and embryo body at E12.5, injected at E6.5 or at E10.5. **d**, Representative images of May-Grünwald-Giemsa stained cytospin preparations of sorted YFP$^+$ and YFP$^-$ CD45$^+$ F4/80^{bright} macrophages of the embryo proper or the head region of E13.5 *Tie2*^{MeriCreMer}*Rosa26*^{YFP} embryos pulsed at E7.5. Scale bar, 10 μm **e**, Quantification of the percentage of YFP$^+$ stem/progenitor cells in the fetal liver and macrophages in yolk sac, brain (head) and embryo body at E12.5. Embryos were labelled at E6.5 ($n = 5$), or E7.5 ($n = 7$), or E8.5 ($n = 4$), or E9.5 ($n = 5$) or E10.5 ($n = 7$) and analysed at E12.5 (mean ± s.d.).

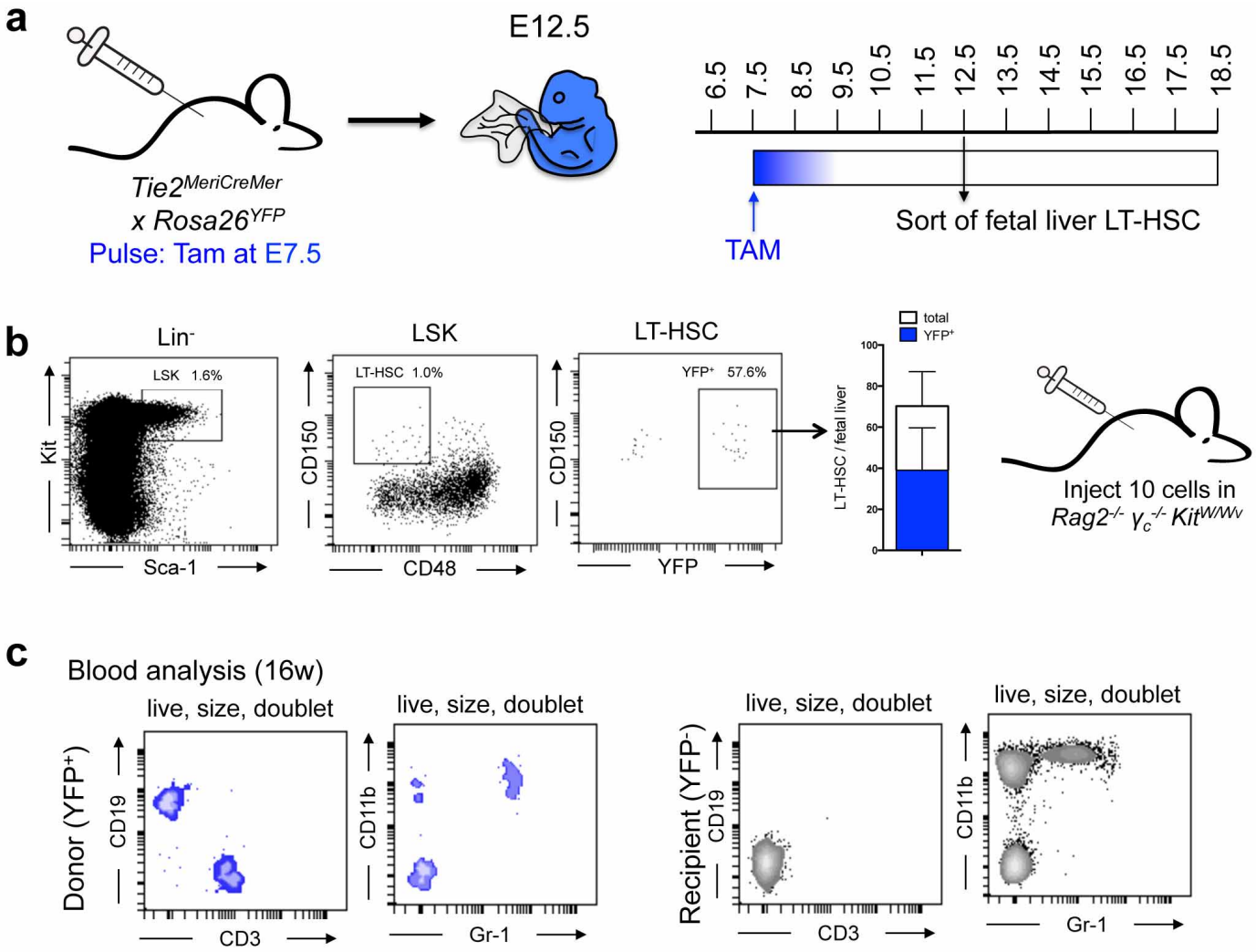

Extended Data Figure 9 | Transplantation of YFP$^+$ fetal liver LT-HSCs from *Tie2^{MeriCreMer}Rosa26^{YFP}* into *Rag2$^{-/-}$γc$^{-/-}$Kit$^{W/Wv}$* mice. **a**, Experimental design for pulse-labelling and LT-HSCs sort from *Tie2^{MeriCreMer}Rosa26^{YFP}* embryos pulsed at E7.5. **b**, Fetal livers of E12.5 embryos pulsed at E7.5 were collected, YFP$^+$LSK CD150$^+$CD48$^-$LT-HSCs were sorted by flow cytometry and 10 LT-HSCs were injected into *Rag2$^{-/-}$γc$^{-/-}$Kit$^{W/Wv}$* recipients. **c**, Blood analysis of recipients 16 weeks after LT-HSC transplantation. Donor-derived (YFP$^+$) and recipient-derived (YFP$^-$) blood cells were analysed for expression of CD19, CD3, CD11b, and Gr-1. One representative example is shown.

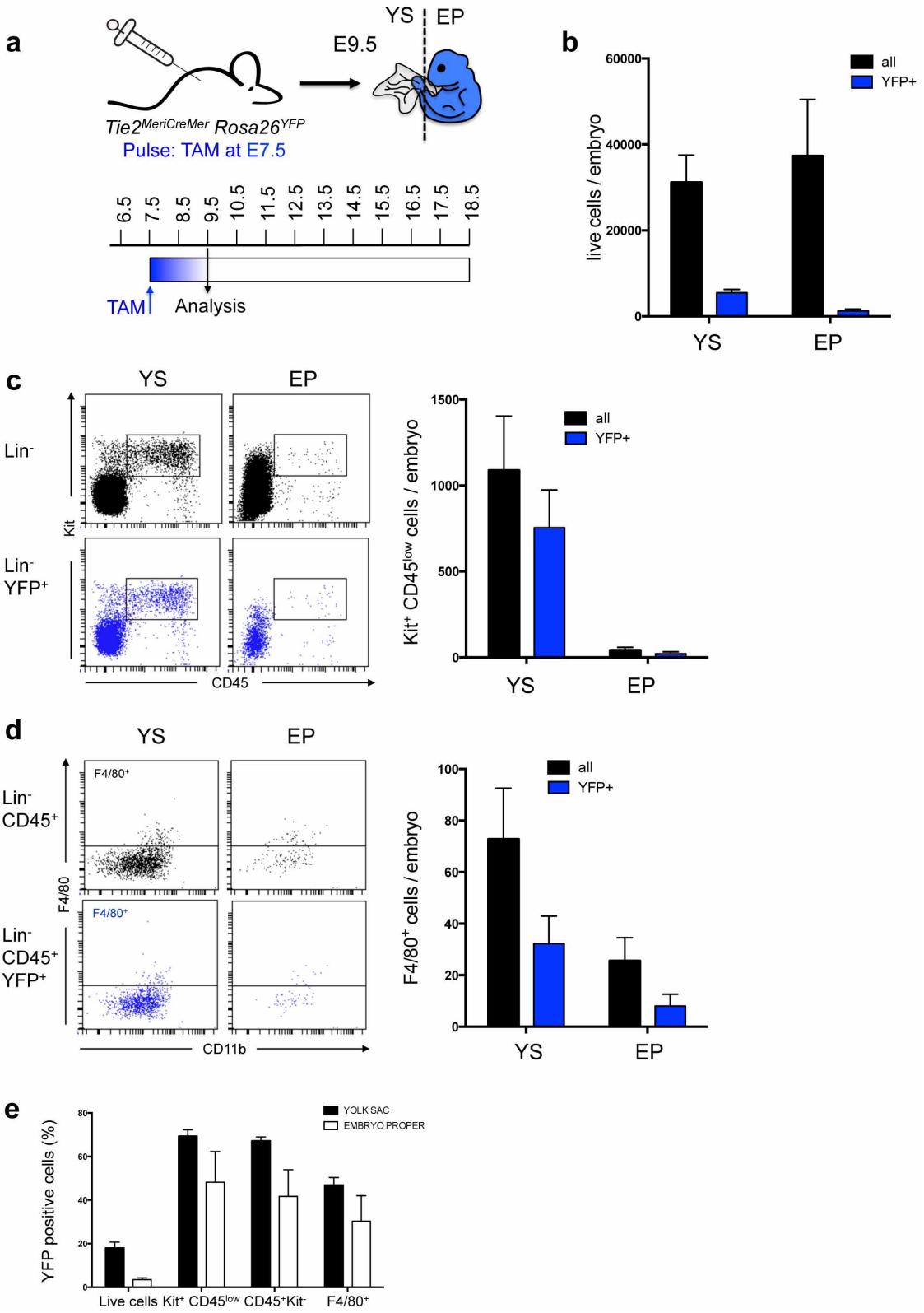

Extended Data Figure 10 | Analysis of E9.5 YS progenitor cells in *Tie2*^{MeriCreMer}*Rosa26*^{YFP} embryos pulse-labelled at E7.5. **a**, Experimental design for fate-mapping analysis of *Tie2*-expressing cells in *Tie2*^{MeriCreMer}*Rosa26*^{YFP} embryos. Embryonic cells were pulse-labelled by tamoxifen (TAM) administration into pregnant *Tie2*^{MeriCreMer} mice at E7.5. Yolk sac (YS) and embryo proper (EP) of E9.5 *Tie2*^{MeriCreMer}*Rosa26*^{YFP} embryos were analysed by flow cytometry. **b**, Quantification of total living cells and YFP$^+$ living cells in yolk sac and embryo proper of analysed embryos (mean ± s.d., $n = 5$). **c**, Flow cytometry analysis of Kit$^+$CD45^{lo} cells among total living cells (black) or living YFP$^+$ cells (blue) in yolk sac and embryo proper of a representative E9.5 *Tie2*^{MeriCreMer}*Rosa26*^{YFP} embryo (left) and quantification of all analysed embryos (right; mean ± s.d., $n = 5$). **d**, Analysis of F4/80$^+$ fetal macrophages among CD45$^+$ cells (black) or YFP$^+$CD45$^+$ cells (blue) in yolk sac and embryo proper (mean ± s.d., $n = 5$) and quantification of all analysed embryos (right; mean ± s.d., $n = 5$). **e**, Percentage of YFP$^+$ cells (YFP labelling efficiency) among live cells, Kit$^+$ CD45^{lo}, CD45$^+$ Kit$^-$ cells and F4/80$^+$ cells from the yolk sac and embryo proper of E9.5 *Tie2*^{MeriCreMer}*Rosa26*^{YFP} embryos pulsed at E7.5.